U.S. Department of Energy
HelioCon
Heliostat Consortium for Concentrating Solar-Thermal Power

Effects of Atmospheric Boundary Layer Turbulence on Single Heliostat Wind Load Coefficients: Comparison of Field Measurements with Wind Tunnel Experiments

Matthew Emes, Matthew Marano, Maziar Arjomandi
The University of Adelaide, Australia

16 July 2024 • ASME ES2024 • Anaheim

conceptual design • components • integration • mass production • heliostat field

Introduction – Heliostat Wind Loads

- Part-depth atmospheric boundary layer (ABL) in wind tunnel experiments limited in scaling both horizontal and vertical turbulence
- Dynamic loads based on streamwise wind speed and turbulence intensity can underestimate wind-induced displacements due to bending moments

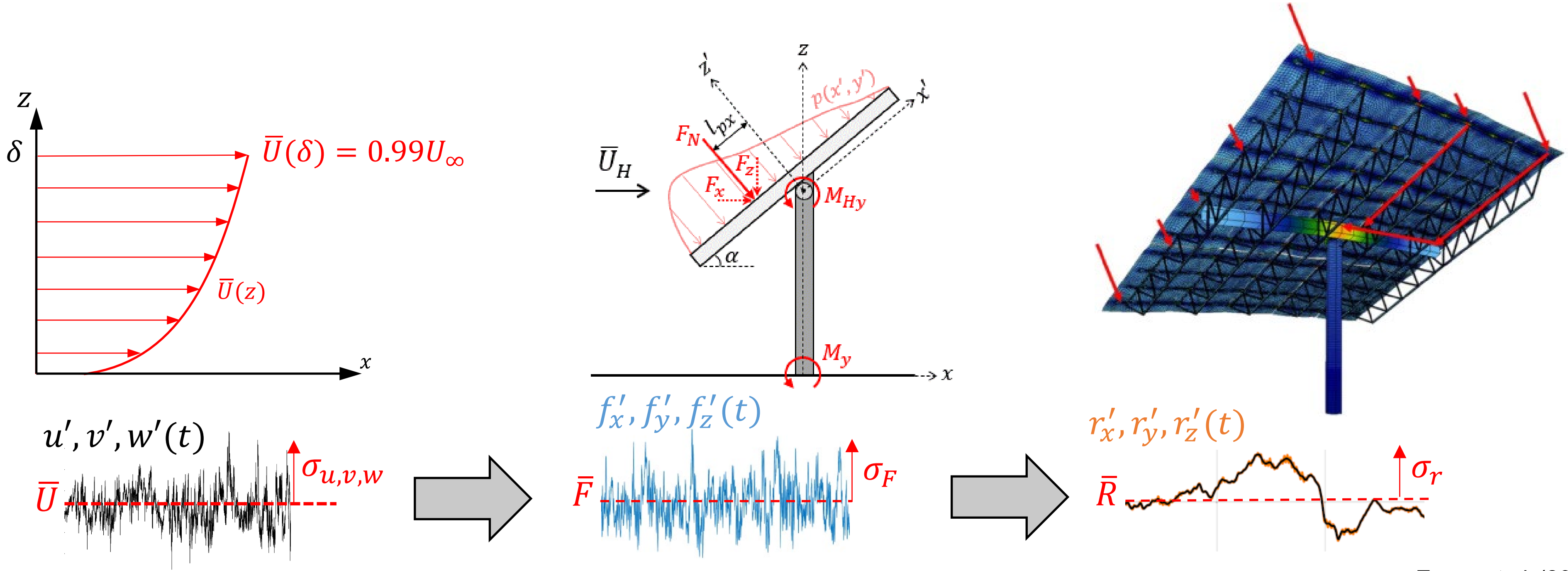

Adapted from Emes *et al.* (2019), von Reeken *et al.* (2016), and Blume *et al.* (2020)

Emes *et al.* (2024), *Journal of Solar Energy Engineering*

Wind tunnel experiments – instrumentation

- 1:114 part-depth ABL
  - Open farmland, grassy plains
- 1:6 scale heliostat model
  - b = 0.33 m, c = 0.53 m, H = 0.25 m
- JR3 six-axis load cell

  ±100 N F_x, F_y, ±200 N F_z, ±12 Nm M_x, M_y, M_z with ±0.25% accuracy
- 24 differential pressure sensors

  ±1” H2O (±248.84 Pa) with ±0.25% accuracy

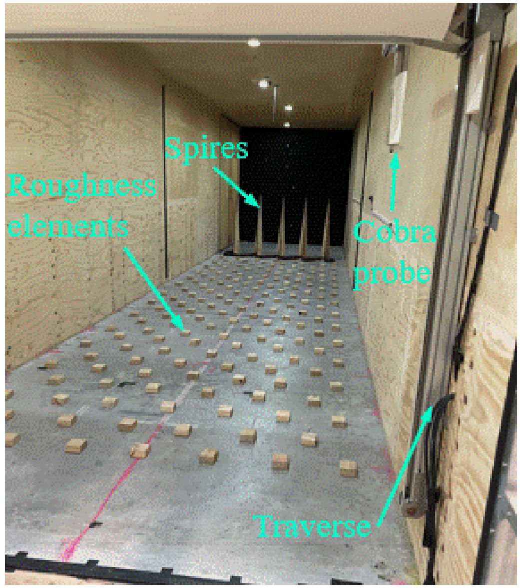

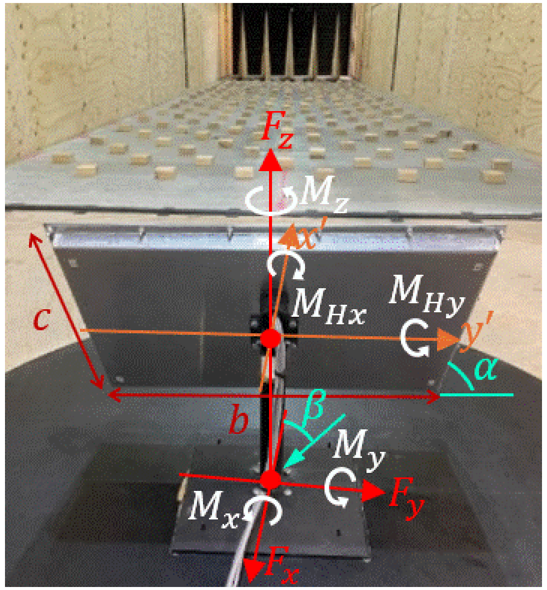

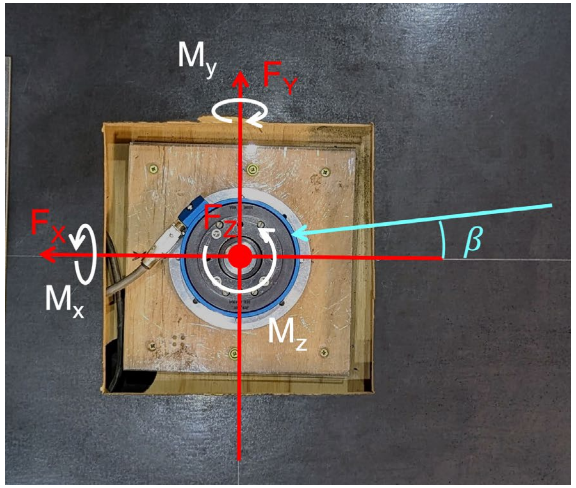

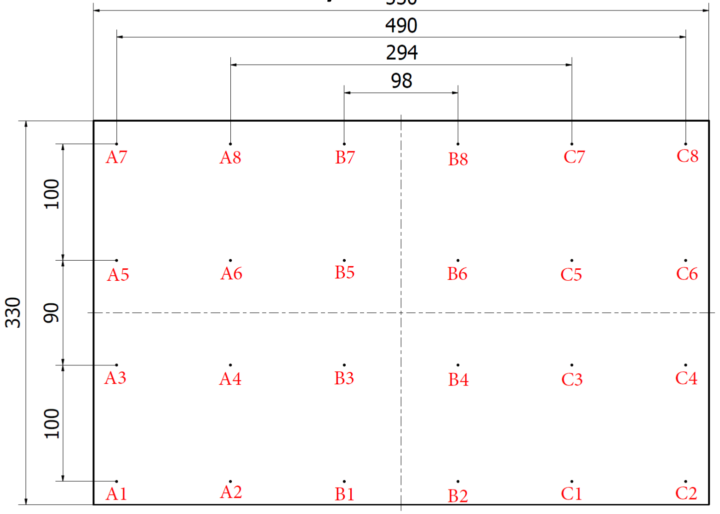

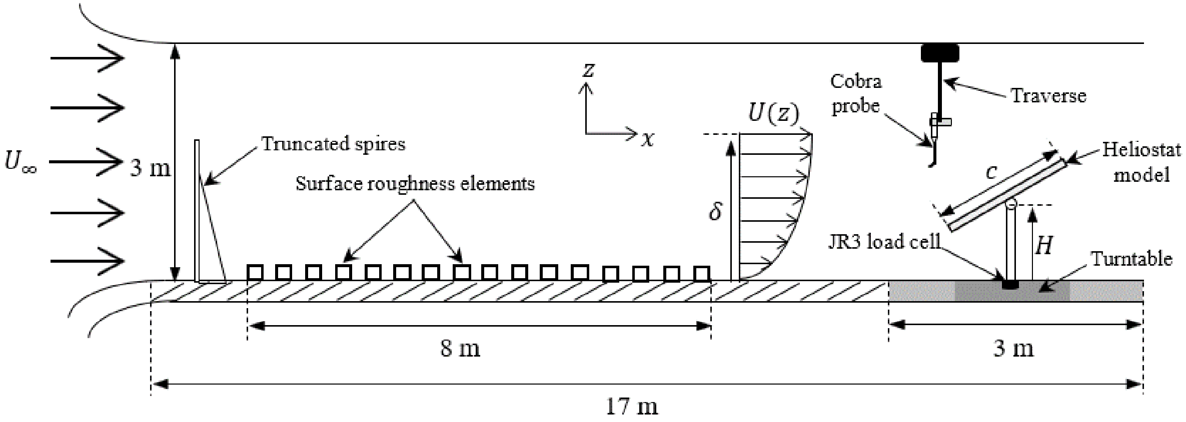

Wind tunnel experiments – ABL profiles

- Mean velocity profile

$$U(z) = \frac{u_\tau}{k}\ln\frac{z}{z_0} + d$$

u_τ = 0.48 m/s, z_0 = 0.01 m, d = 4.4

$$U(z) = U_\infty\left(\frac{z}{\delta}\right)^{\alpha}$$

U_∞ = 11.8 m/s, δ = 1.3 m, α = 0.35

- Turbulence intensity profiles

z_0 = 0.01 m (ESDU 85020)

- Turbulence length scales

z_0 = 0.01 m (ESDU 85020)

α = 0.35 (ESDU 74031)

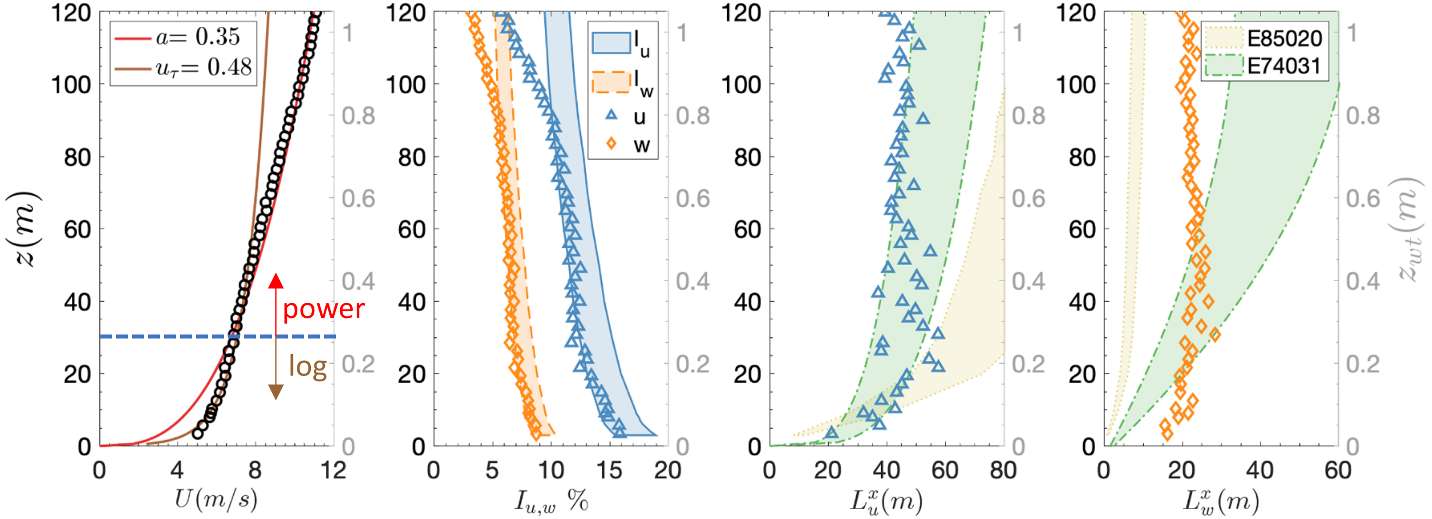

Marano et al. (2024), *Solar Energy*

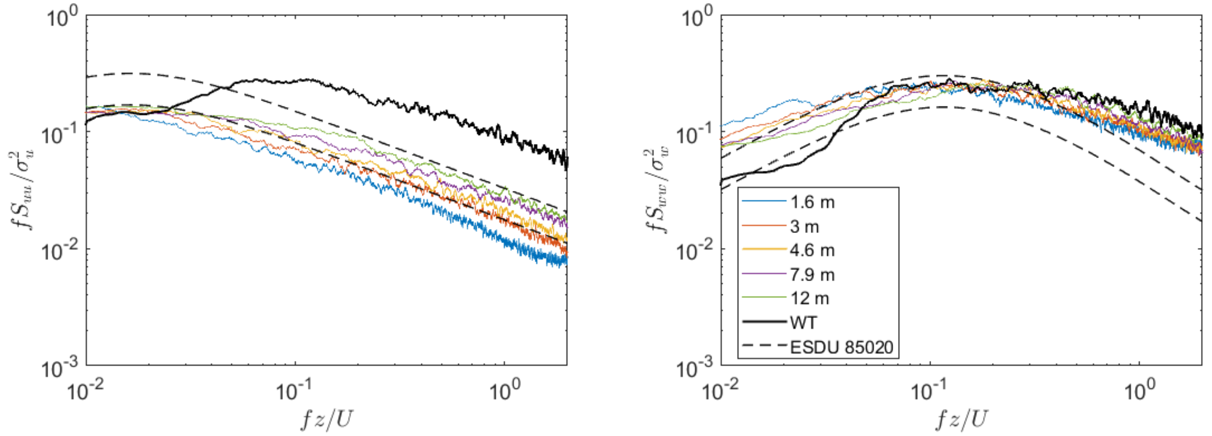

Emes et al. (2024), *Solar Energy* (under review)

ABLRF – layout

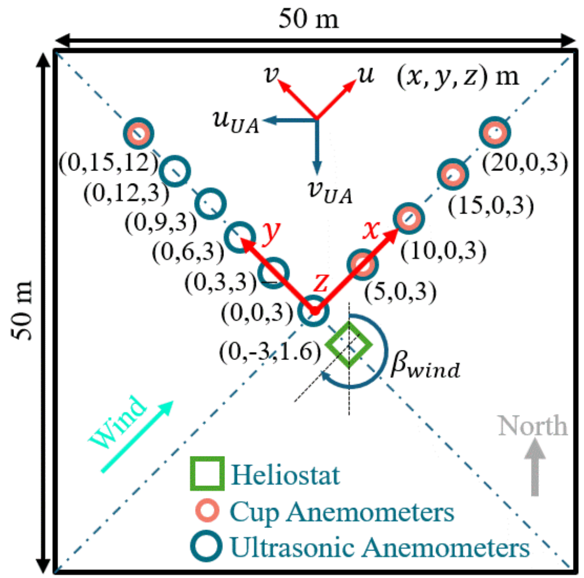

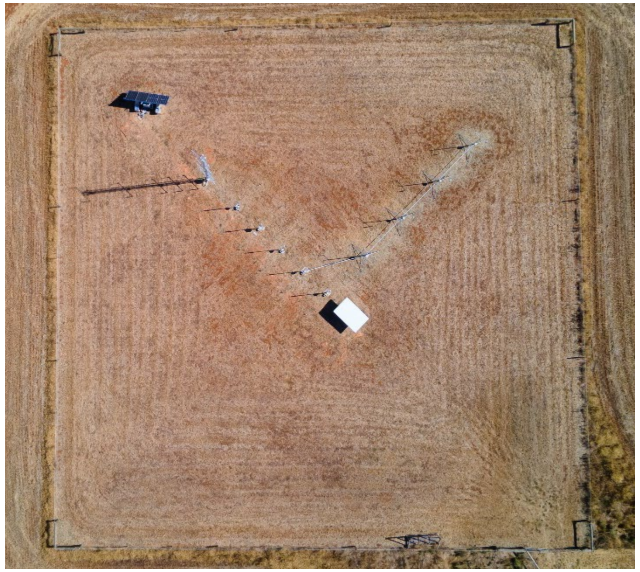

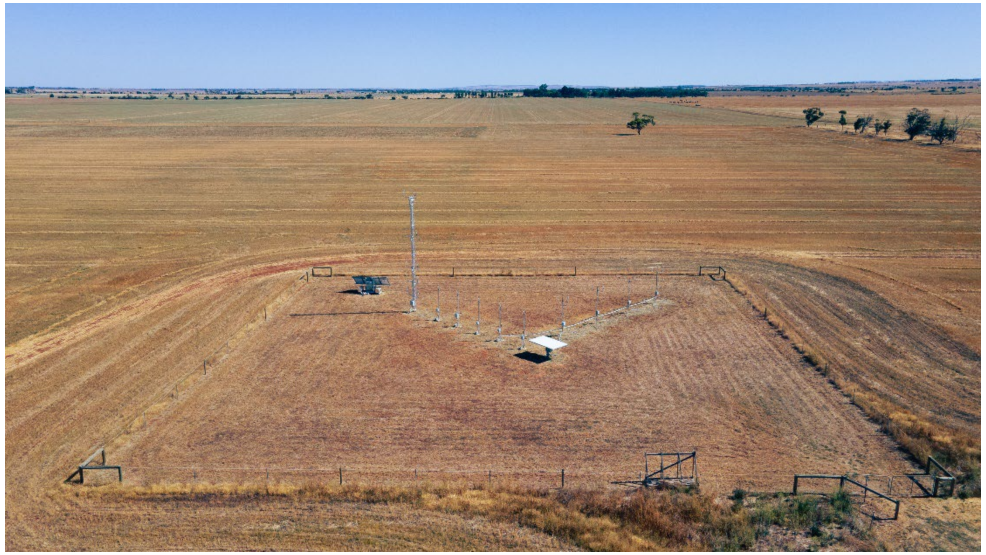

- 14 ultrasonic anemometers
- 9 cup anemometers
- Open farmland

ABLRF – instrumentation

- Campbell Scientific 81005A 3D ultrasonic anemometers
  - $\pm$ 0.05 m/s accuracy
  - 0.01 m/s resolution
  - $\pm$ 2°C accuracy
  - 0.01°C resolution
- Risø P2546A cup anemometers
- 48 Honeywell HSC series differential pressure sensors
  - ±0.25% accuracy
  - ±600 Pa measurement range
- ME Systeme K6D175 six-axis load cell
  - ± 0.5% accuracy
  - ± 10 kN F_x, F_y, ± 20 kN F_z
  - ± 1 kNm M_{Hx}, M_{Hy}, ± 2 kNm M_z
- Single industrial computer, 4G modem, four 315 W photovoltaic panels and six 200 Ah batteries

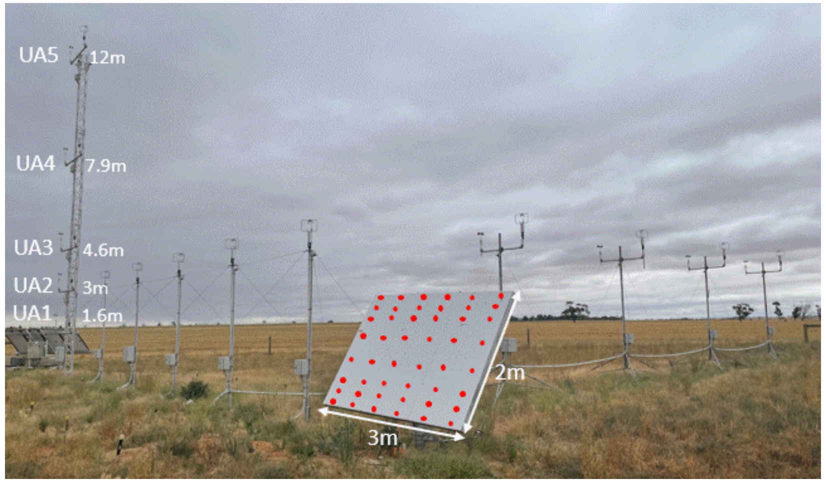

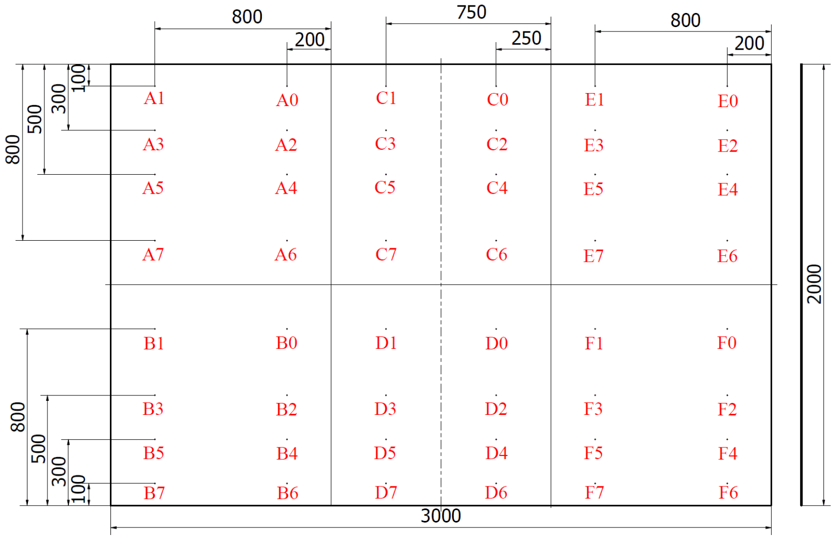

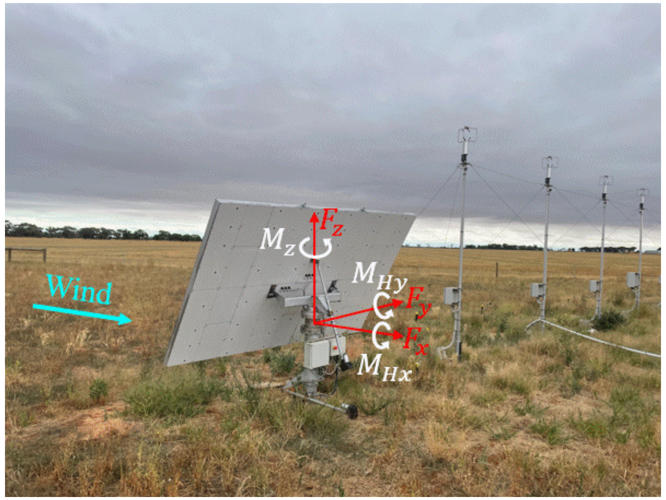

ABL Wind Turbulence Analysis

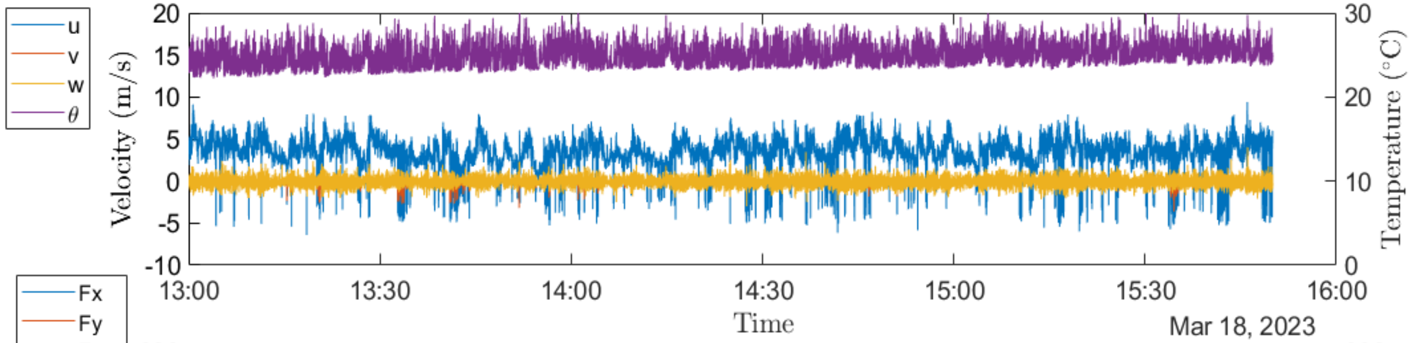

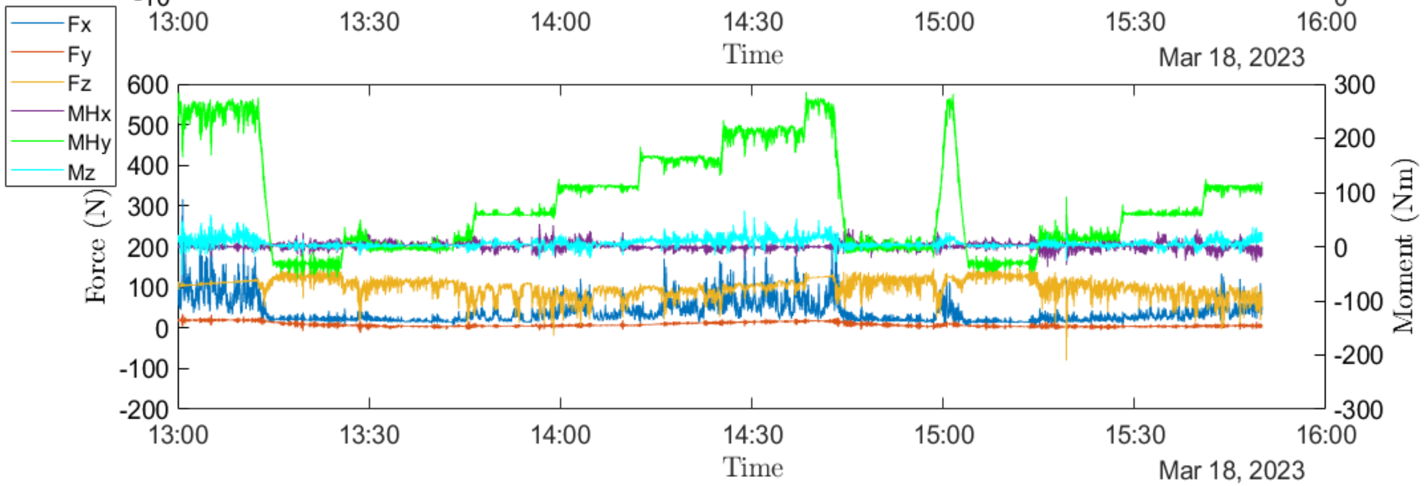

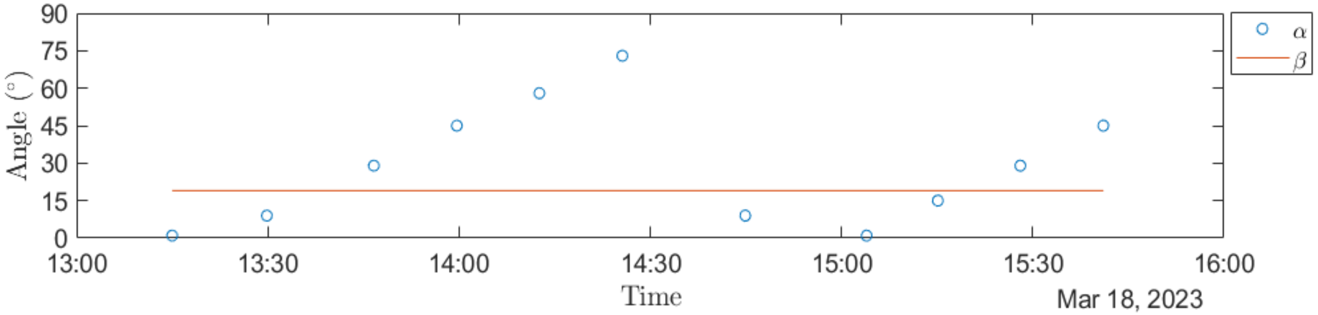

$\beta = 0°$

Wind from SW (225°)

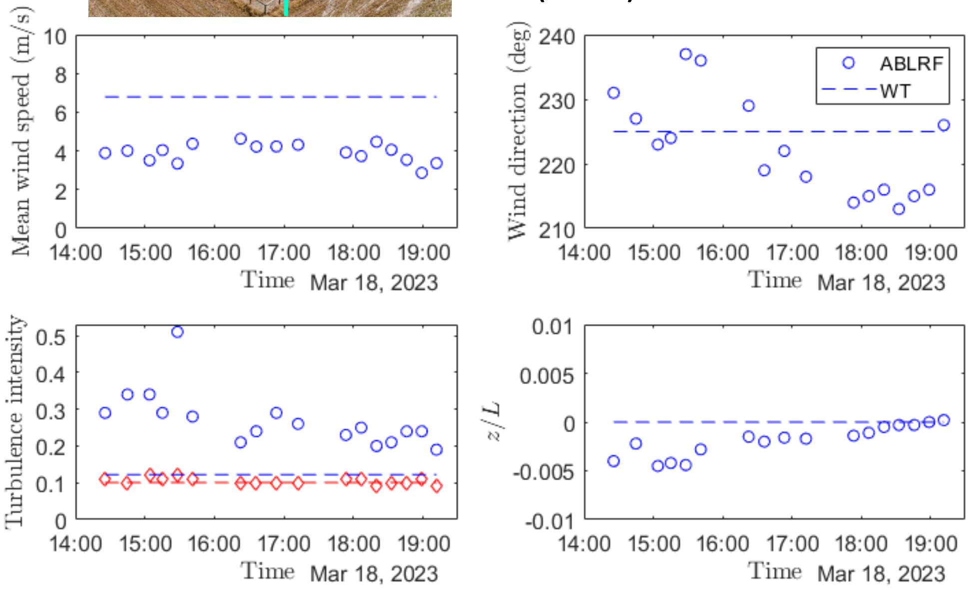

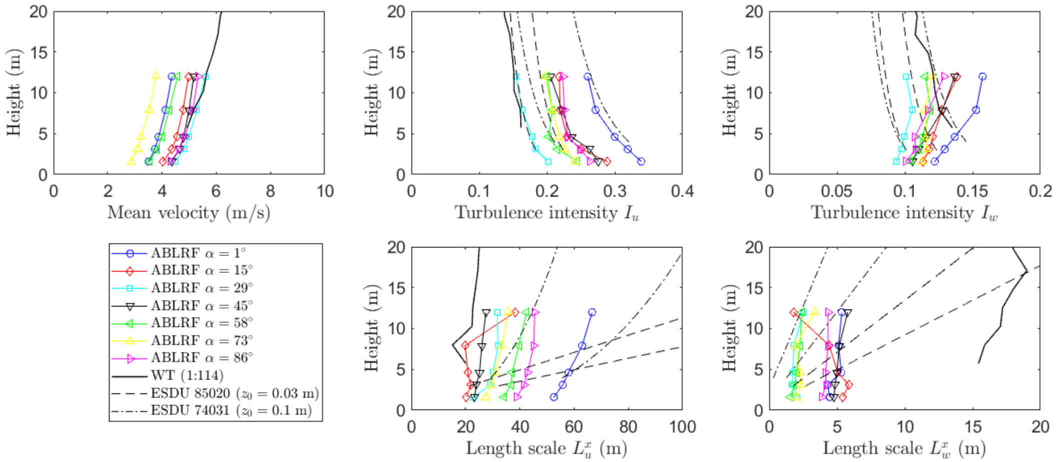

Heliostat Wind Load Analysis

- Drag force and azimuth moment coefficients from load cell (LC) are consistent
- Lift force and hinge moment coefficients from pressure sensors (PS) are consistent but more than 50% difference from LC at $\alpha \leq 30°$
- Influence of L_w^x/c greater than I_u and I_w
- Peak loads sufficiently estimated by a fitted Gaussian distribution

$\beta = 0°$

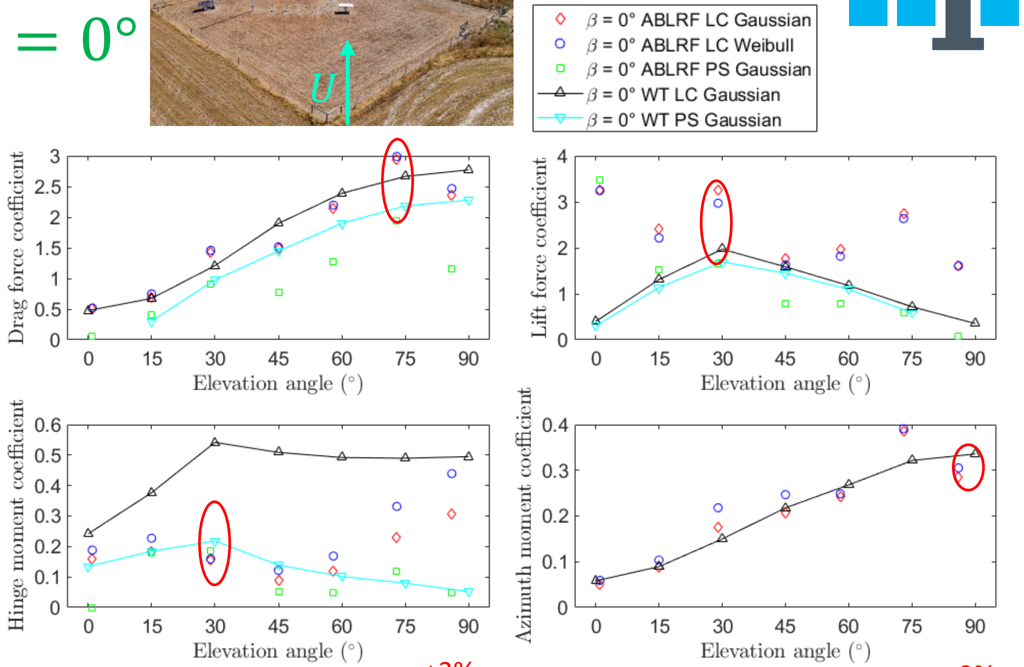

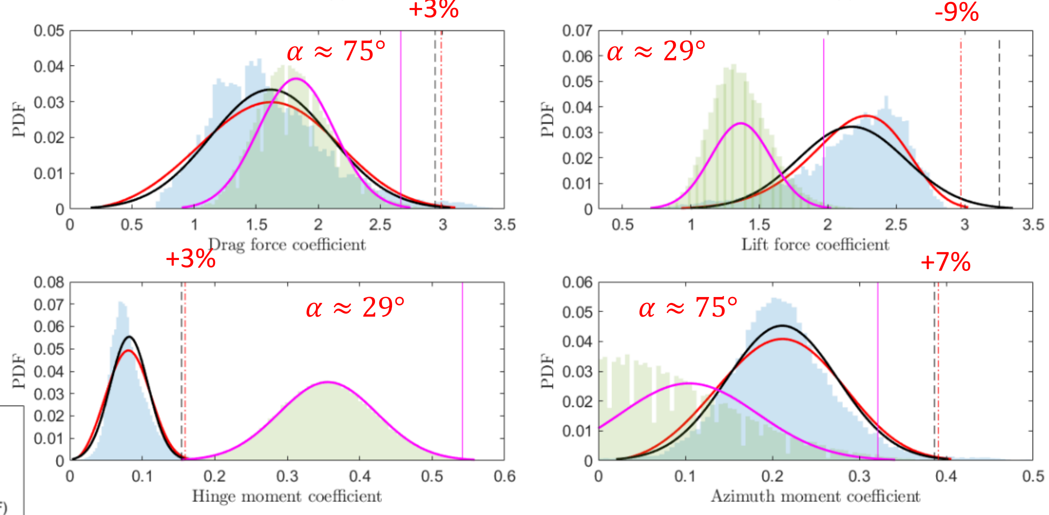

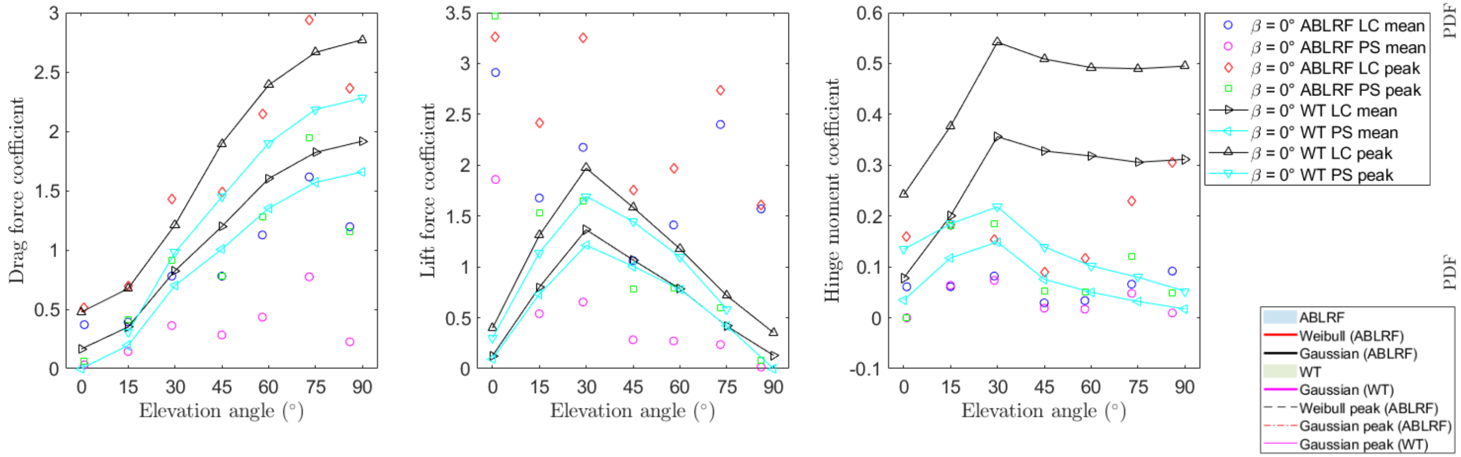

Heliostat Pressure Analysis

- Mean pressure distributions

  $\beta = 0°$

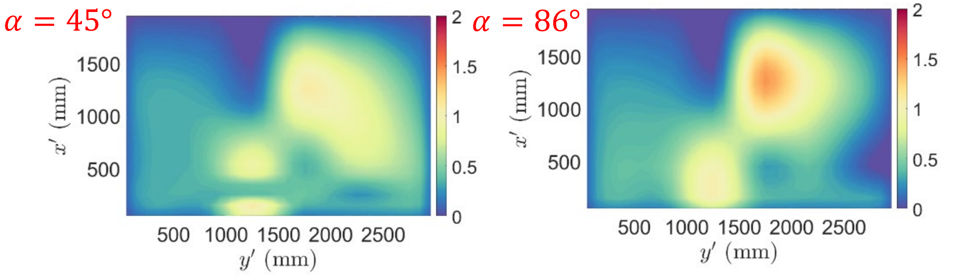

α (°)	Coefficient	Mean CFx	Peak CFx	Mean CFz	Peak CFz	Mean CMHy	Peak CMHy
1	ABLRF	0.03	0.06	1.86	3.47	0	0
0	WT	0	0	0.01	0.38	0.02	0.24
15	ABLRF	0.14	0.41	0.54	1.53	0.06	0.18
15	WT	0.20	0.33	0.73	1.22	0.11	0.19
29	ABLRF	0.36	0.91	0.65	1.65	0.07	0.18
30	WT	0.63	0.93	1.09	1.62	0.10	0.17
45	ABLRF	0.28	0.78	0.28	0.78	0.02	0.05
45	WT	0.98	1.48	0.98	1.48	0.06	0.13
58	ABLRF	0.43	1.28	0.27	0.80	0.02	0.05
60	WT	1.26	1.87	0.73	1.08	0.04	0.09
73	ABLRF	0.77	1.95	0.24	0.60	0.05	0.12
75	WT	1.50	2.20	0.40	0.59	0.02	0.08
86	ABLRF	0.23	1.15	0.02	0.08	0.01	0.05
90	WT	1.48	2.19	0	0	0.01	0.07

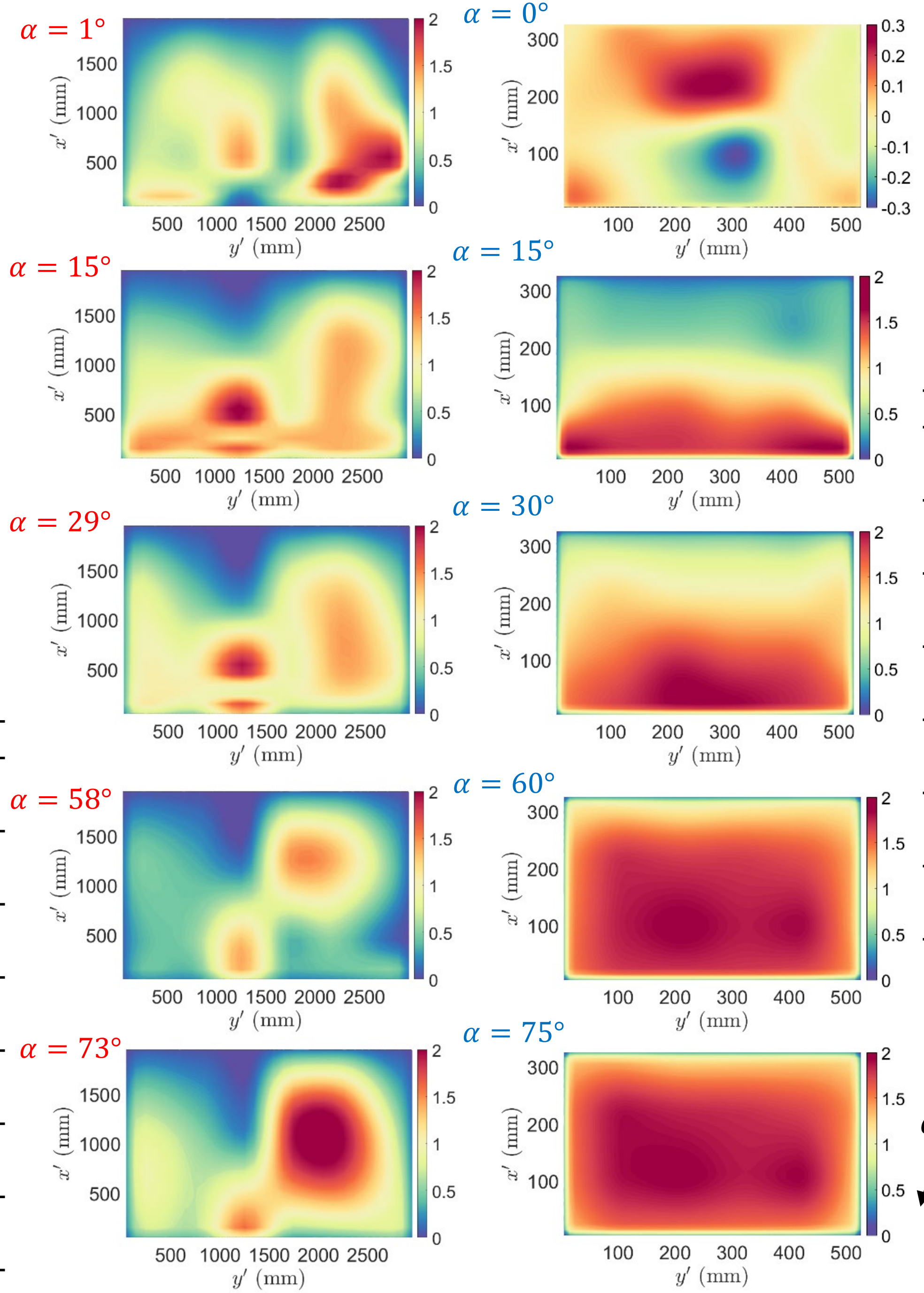

α (°)	Lpx/c	Lpy/b
1	0.50	0.58
0	0.28	0.12
15	0.39	0.53
15	0.35	0.49
29	0.40	0.52
30	0.42	0.50
45	0.45	0.56
45	0.46	0.50
58	0.47	0.54
60	0.47	0.50
73	0.44	0.56
75	0.49	0.49
86	0.46	0.46
90	0.50	0.49

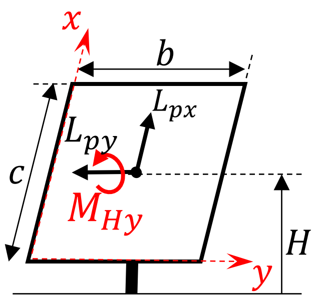

ABL Wind Turbulence Analysis

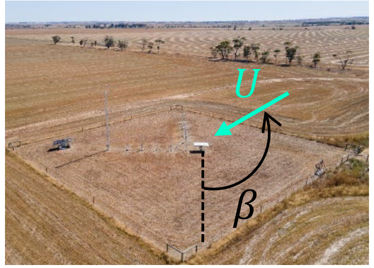

$\beta = 120°$

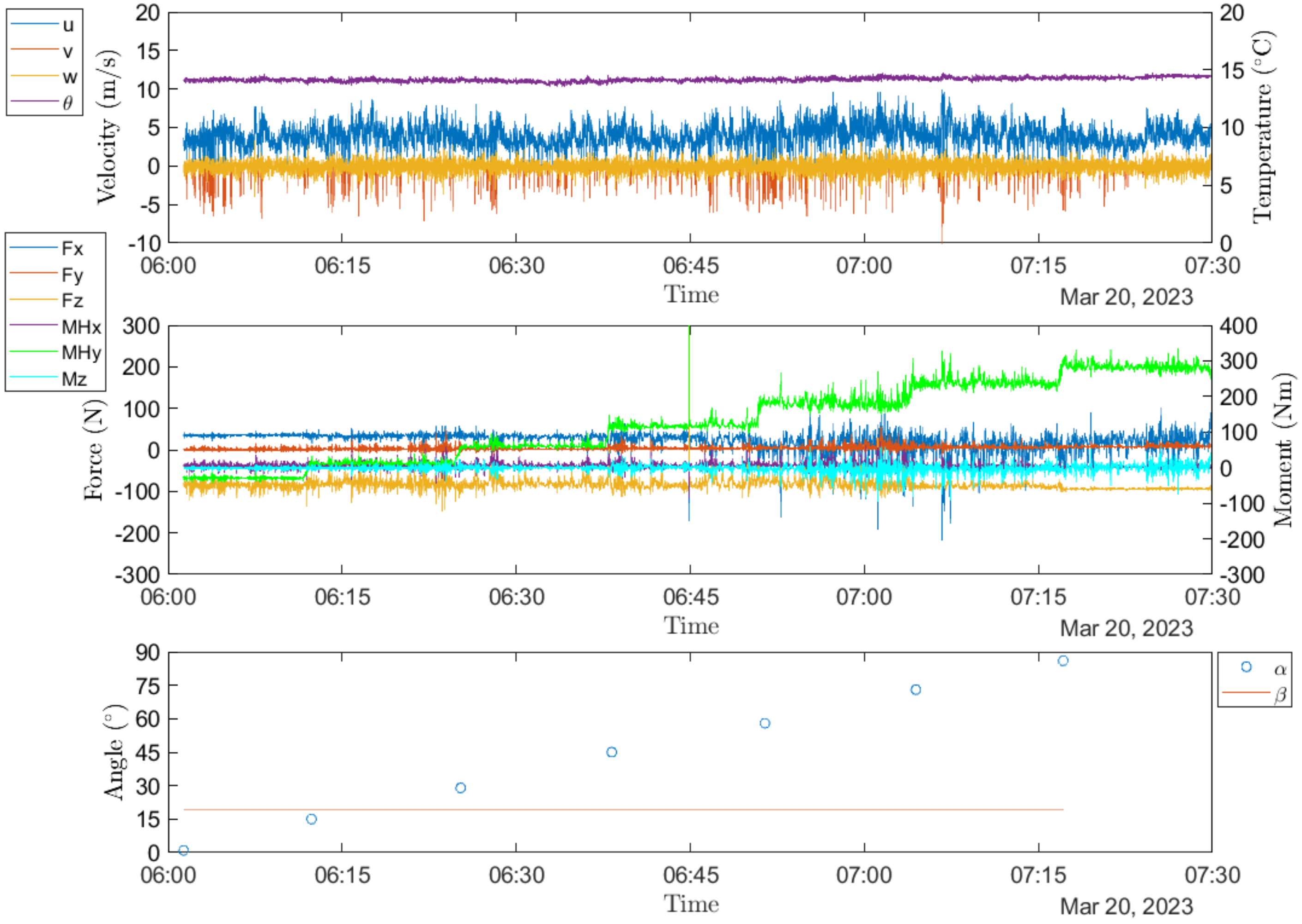

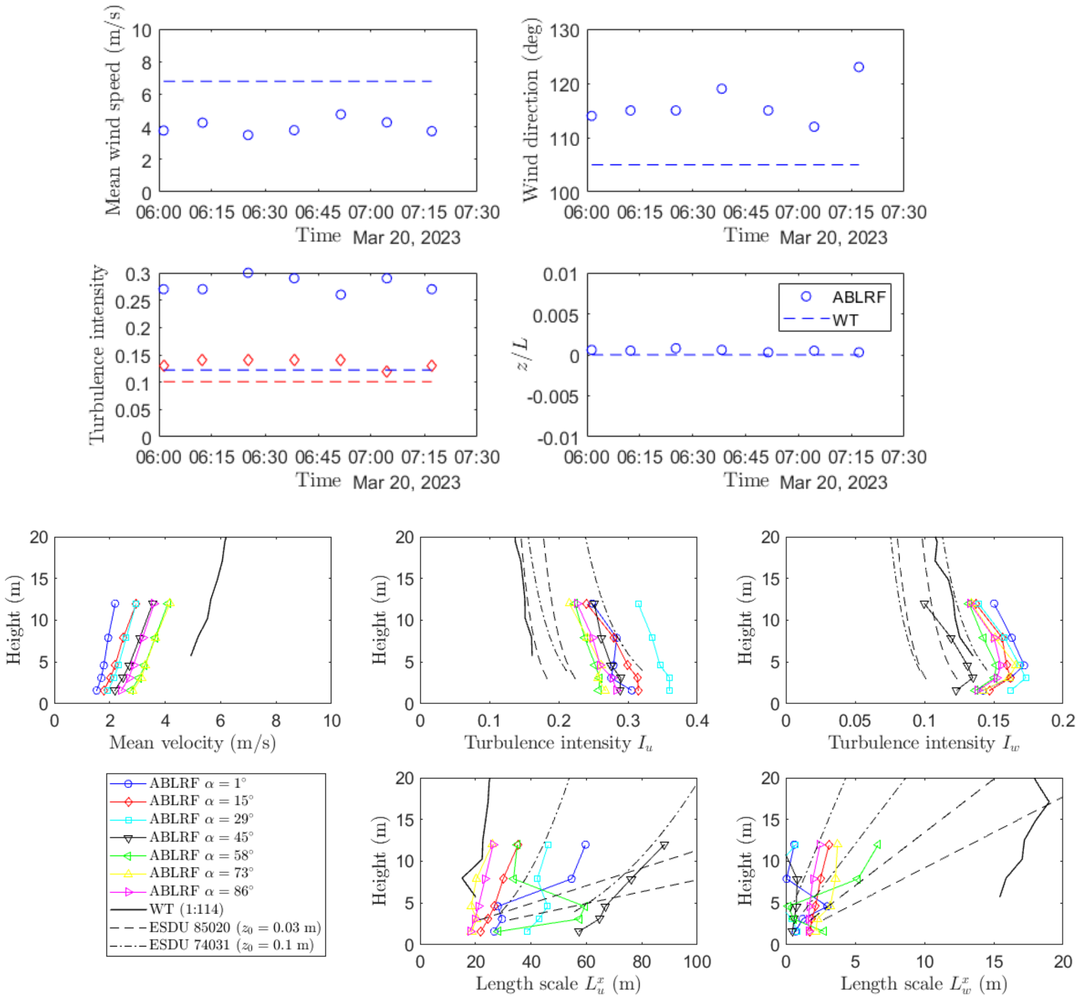

Heliostat Wind Load Analysis

- Drag forces and azimuth moments overestimated in wind tunnel (WT) due to smaller $L_u^x/c \approx 1.3$ (10-15 ABLRF) and despite smaller I_u 12% (26-36% ABLRF)
- Lift forces underestimated in wind tunnel (WT) due to smaller $L_w^x/c \approx 0.53$ (0.4-1.3 ABLRF) and smaller I_w 11% (12-16% ABLRF)

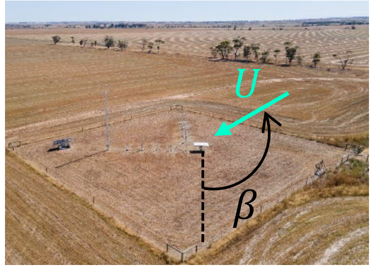

$\beta = 120°$

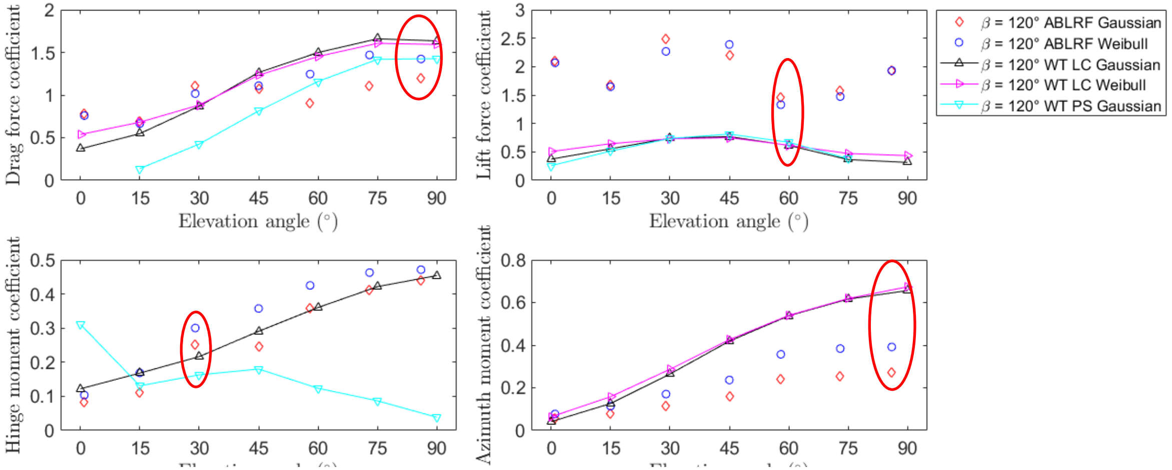

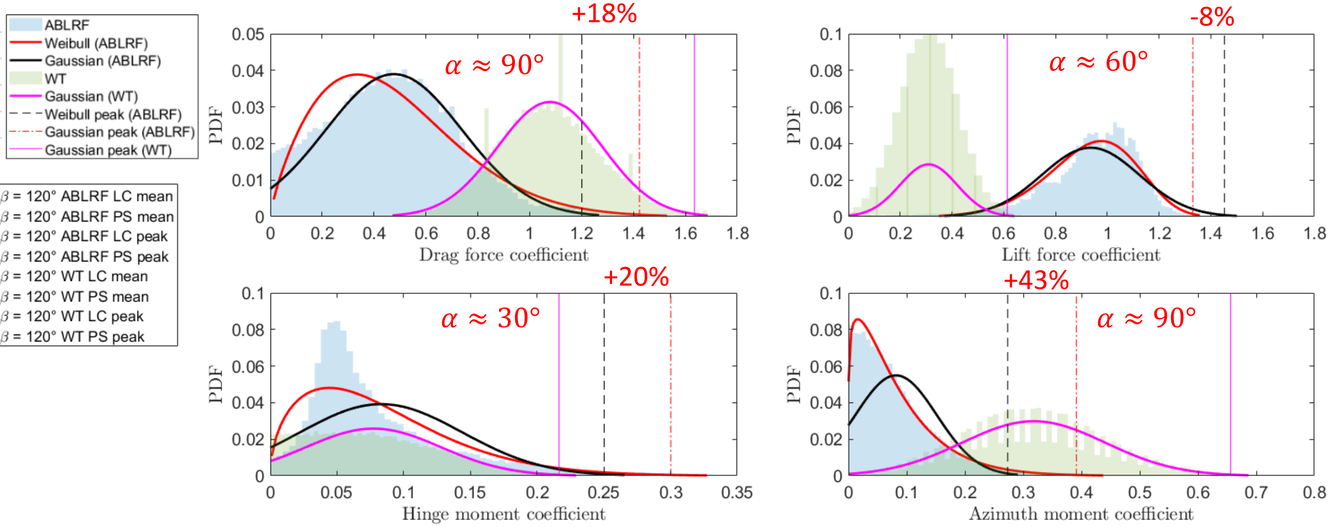

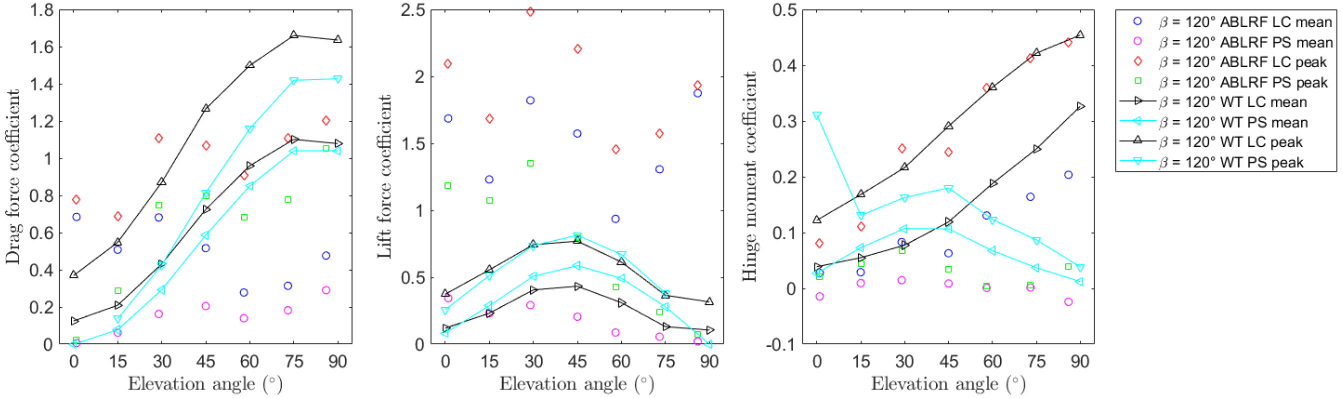

Heliostat Pressure Analysis

- Mean pressure distributions

$\beta = 120°$

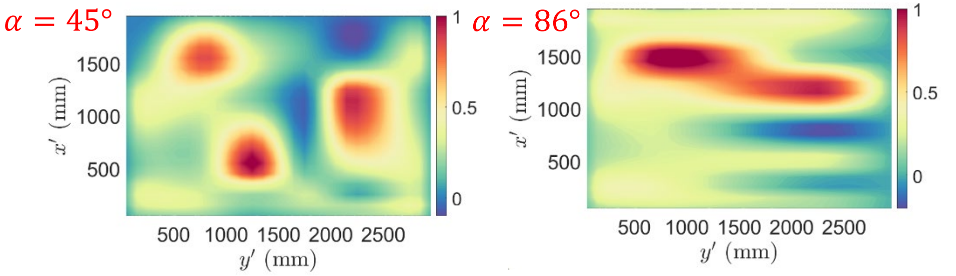

α (°)	Coefficient	Mean CFx	Peak CFx	Mean CFz	Peak CFz	Mean CMHy	Peak CMHy
1	ABLRF	0.01	0.02	0.34	1.18	0.01	0.02
0	WT	0	0	0.00	0.32	0.02	0.34
15	ABLRF	0.06	0.28	0.23	1.07	0.01	0.04
15	WT	0.08	0.14	0.28	0.53	0.07	0.14
29	ABLRF	0.16	0.75	0.29	1.35	0.01	0.07
30	WT	0.29	0.44	0.51	0.76	0.11	0.17
45	ABLRF	0.20	0.80	0.20	0.80	0.01	0.03
45	WT	0.59	0.83	0.59	0.83	0.11	0.19
58	ABLRF	0.14	0.68	0.09	0.43	0.00	0.01
60	WT	0.85	1.19	0.49	0.69	0.07	0.13
73	ABLRF	0.18	0.78	0.06	0.24	0.00	0.01
75	WT	1.03	1.45	0.28	0.39	0.04	0.09
86	ABLRF	0.29	1.05	0.02	0.07	0.02	0.04
90	WT	1.04	1.46	0	0	0.00	0.05

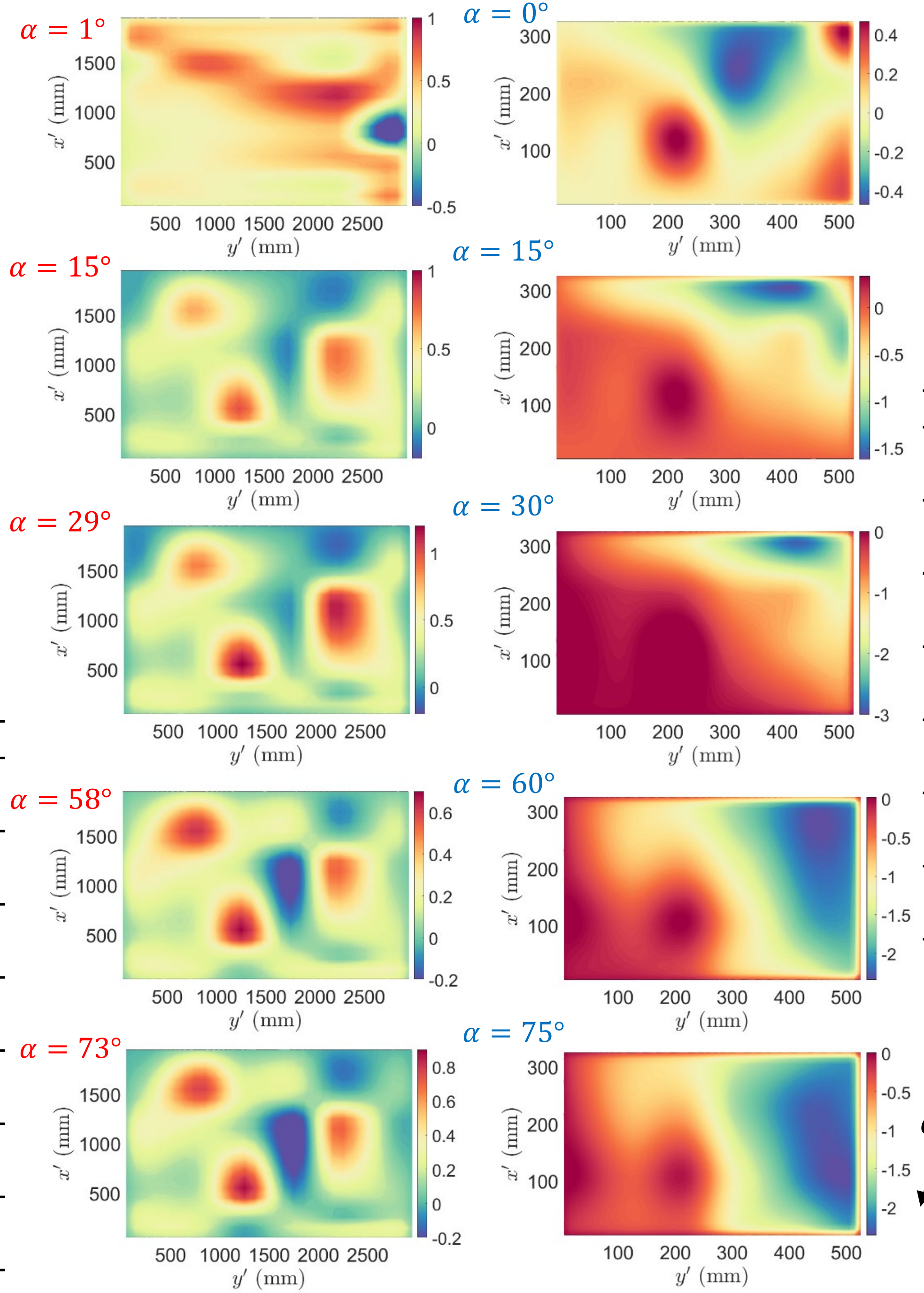

α (°)	Lpx/c	Lpy/b
1	0.54	0.51
0	0.59	0.33
15	0.46	0.51
15	0.77	0.72
29	0.46	0.51
30	0.68	0.71
45	0.47	0.49
45	0.63	0.69
58	0.49	0.44
60	0.57	0.67
73	0.49	0.43
75	0.53	0.67
86	0.58	0.43
90	0.50	0.67

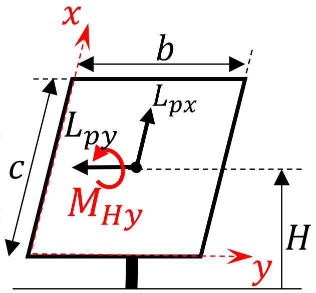

ABL Wind Analysis

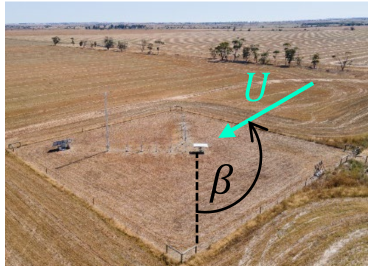

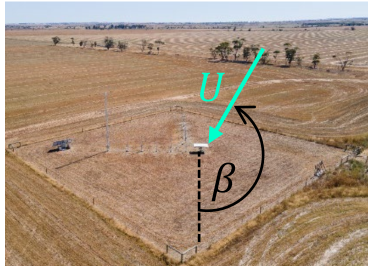

$\beta = 120°$

$\beta = 150°$

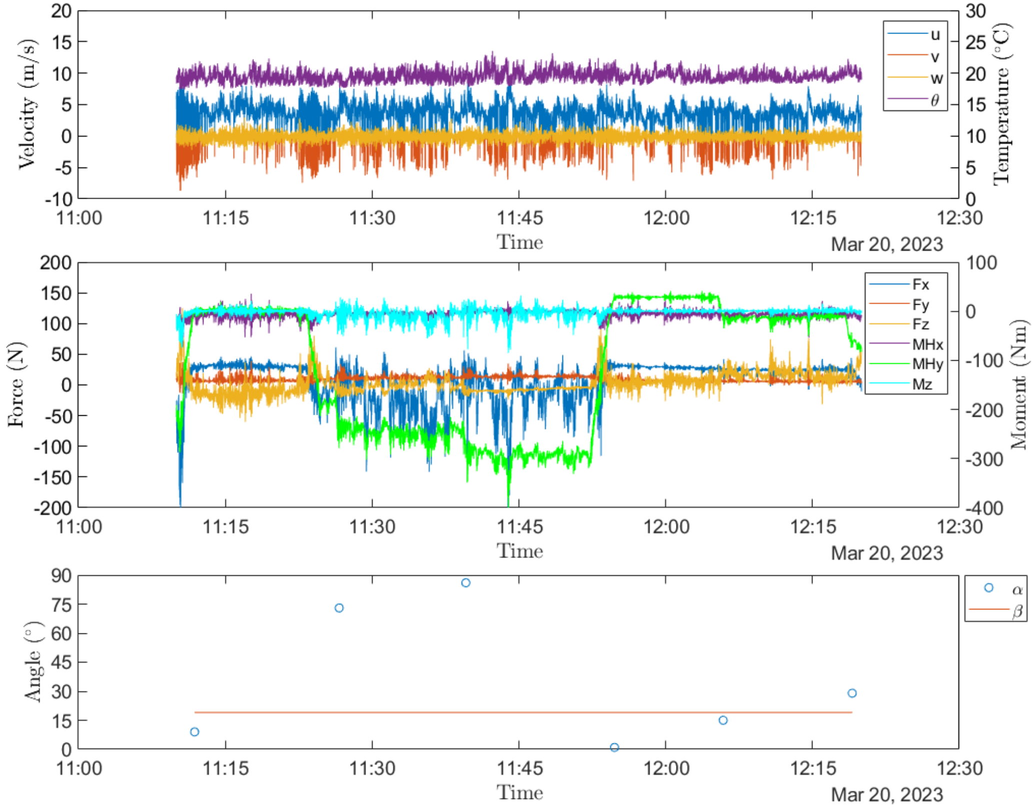

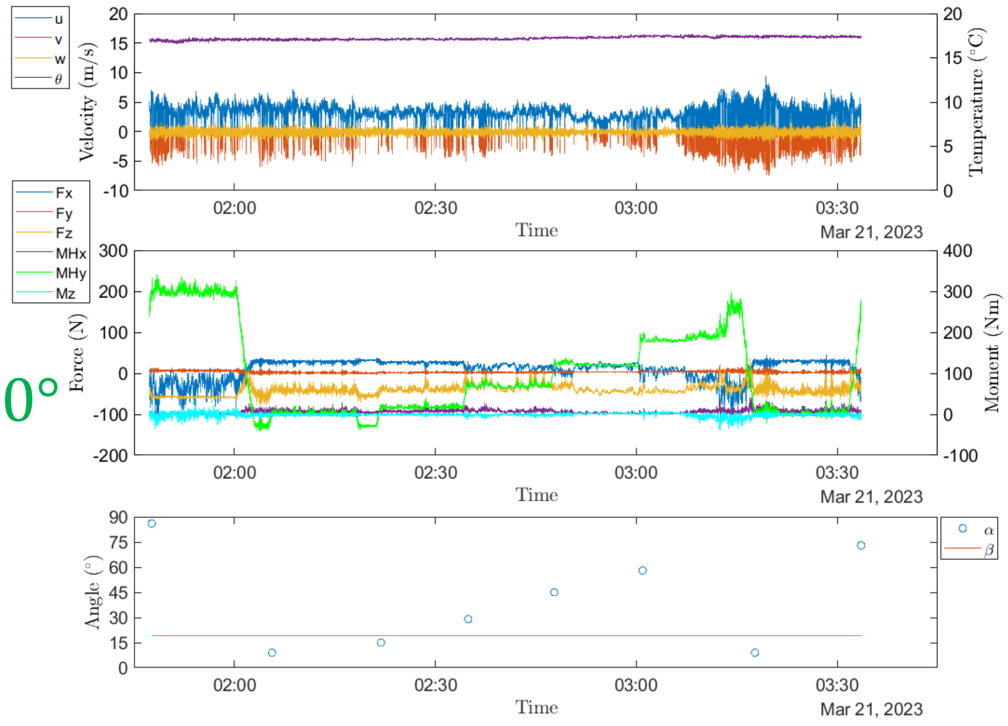

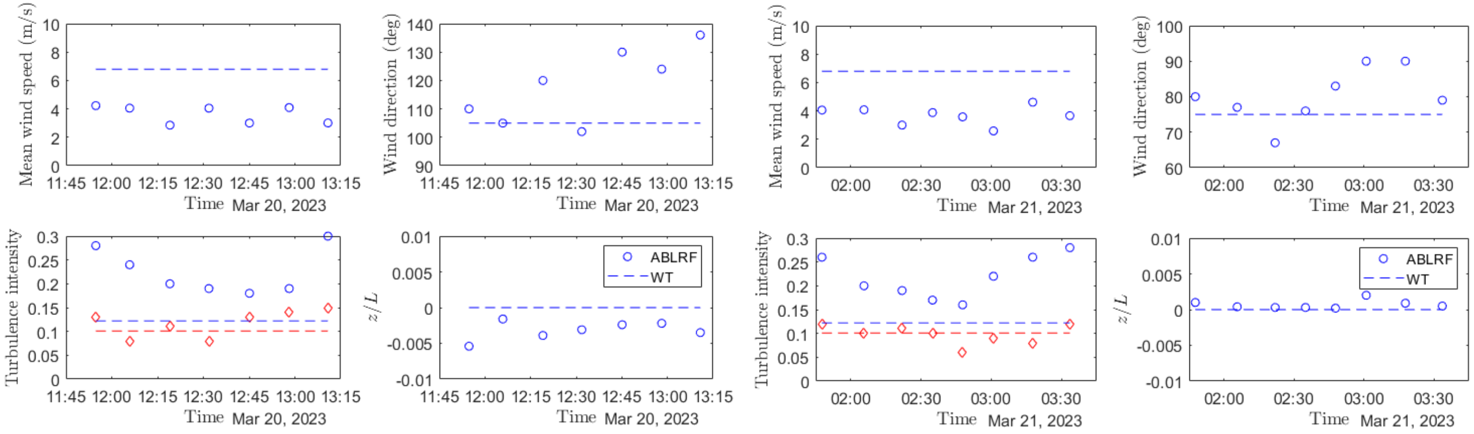

ABL Turbulence Analysis

$\beta = 120°$

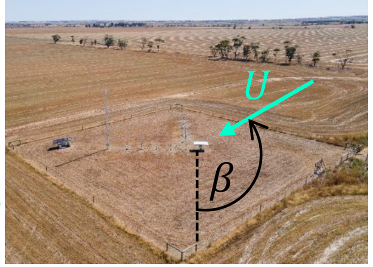

$\beta = 150°$

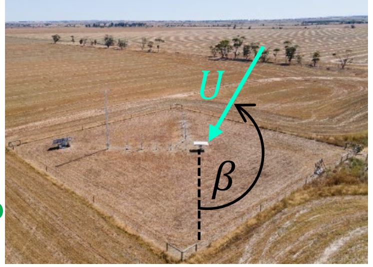

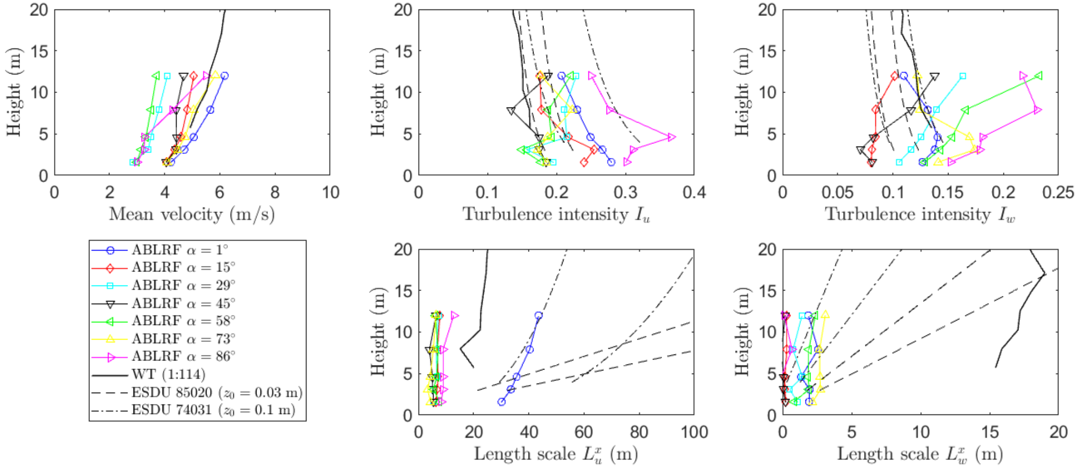

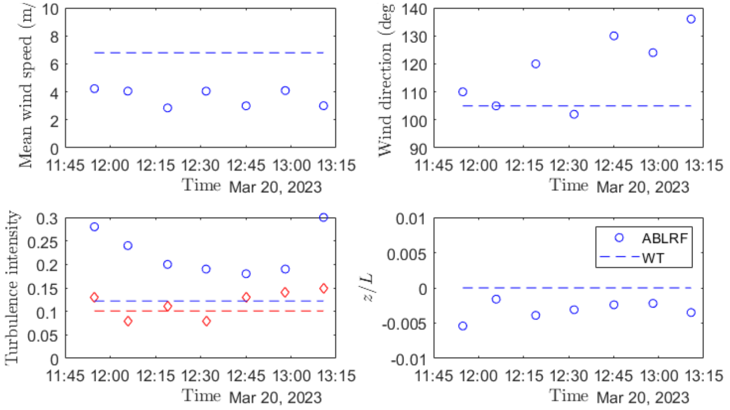

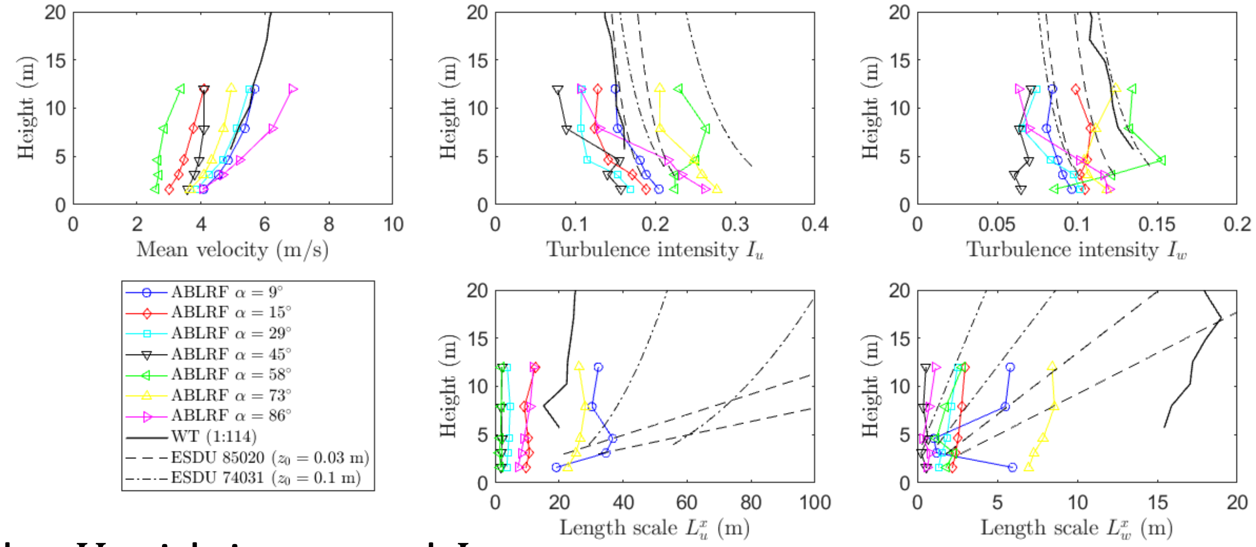

- Similar U with increased I_w and decreased L_w^x in early afternoon compared to early morning

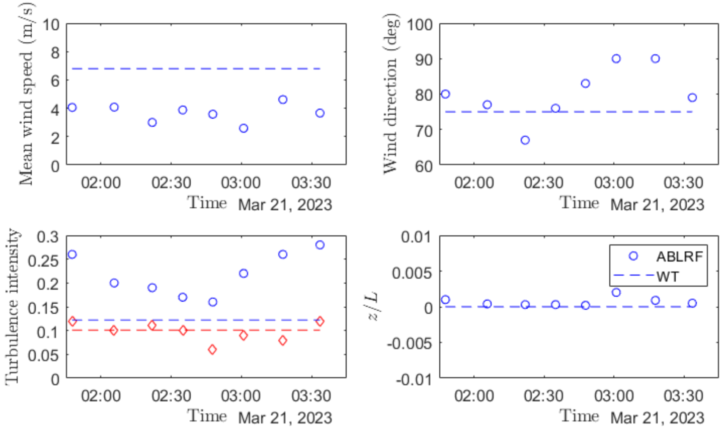

- Large scatter in β, L_u^x and L_w^x at different α for constant facing direction (SW 225°)
- Sensitivity of L_u^x and L_w^x and wind spectra to atmospheric stability

Heliostat Wind Load Analysis

$\beta = 120°$

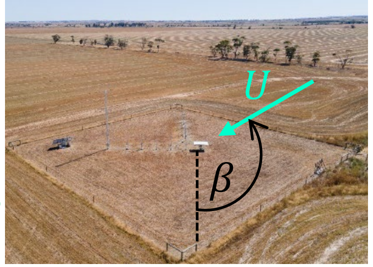

$\beta = 150°$

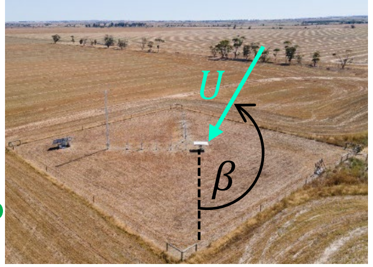

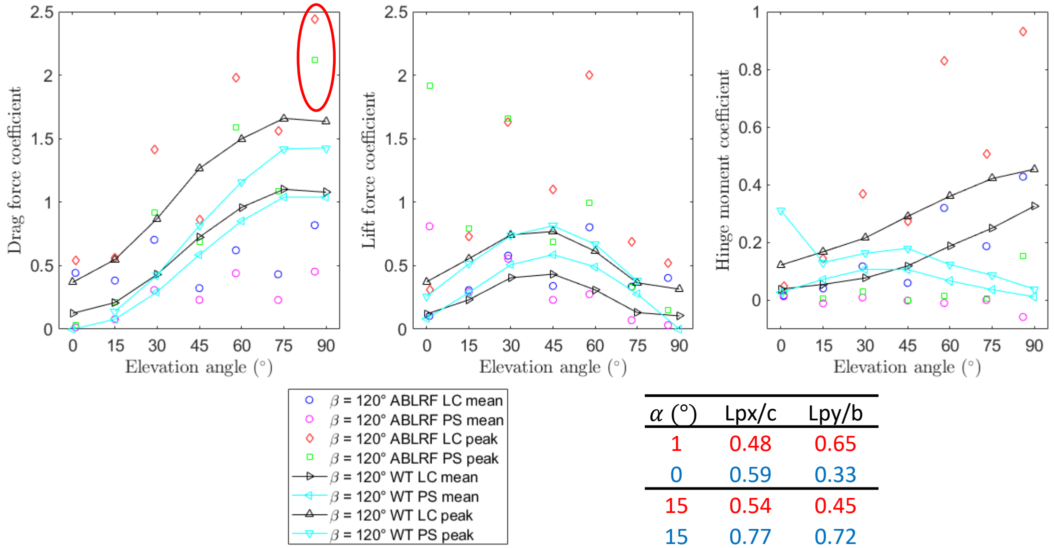

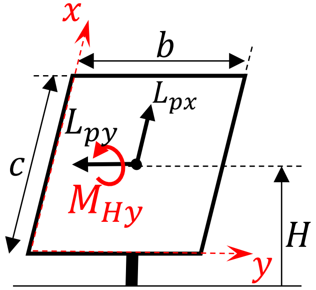

α (°)	Lpx/c	Lpy/b
1	0.48	0.65
0	0.59	0.33
15	0.54	0.45
15	0.77	0.72
29	0.48	0.49
30	0.68	0.71
45	0.50	0.46
45	0.63	0.69
58	0.52	0.41
60	0.57	0.67
73	0.50	0.43
75	0.53	0.67
86	0.63	0.41
90	0.50	0.67

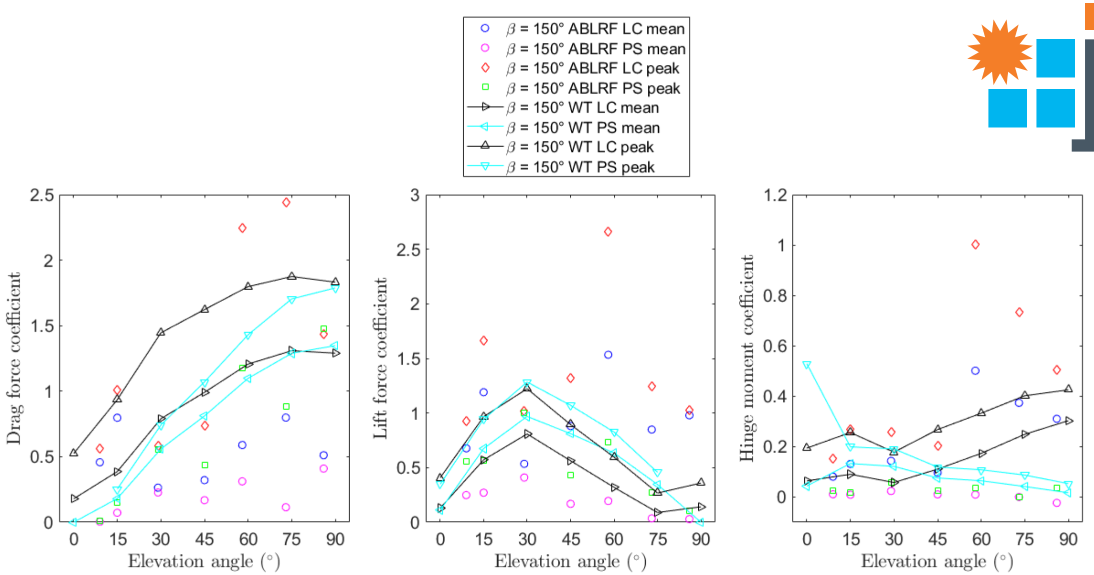

- Peak **drag force and azimuth moment** at $\alpha = 86°$ ($\beta \approx 120°$) increase by factors of **2 and 1.85** respectively with increasing I_u 28% to 30% and decreasing L_u^x/c 9 to 2 at ABLRF

α (°)	Lpx/c	Lpy/b
15	0.47	0.47
15	0.69	0.64
29	0.45	0.45
30	0.61	0.60
45	0.46	0.46
45	0.57	0.58
58	0.47	0.40
60	0.55	0.58
73	0.50	0.17
75	0.53	0.58
86	0.56	0.44
90	0.51	0.59

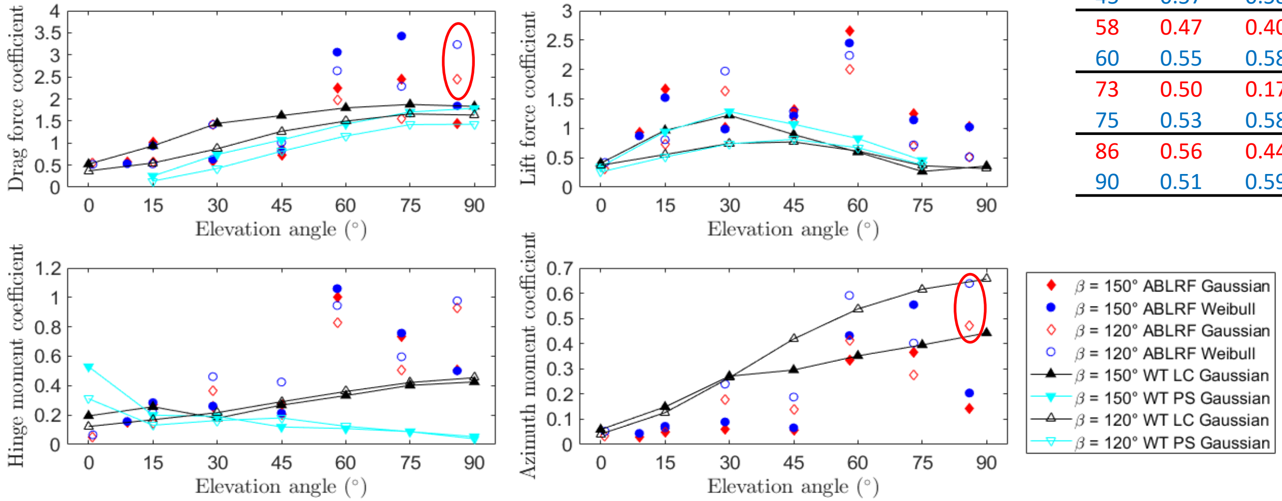

Heliostat Wind Load Analysis

$\beta = 120°$

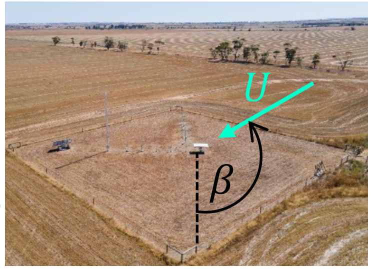

$\beta = 150°$

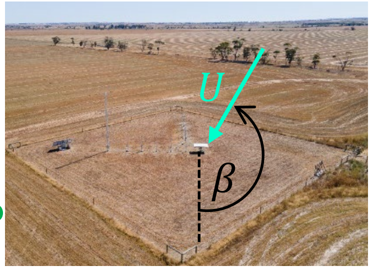

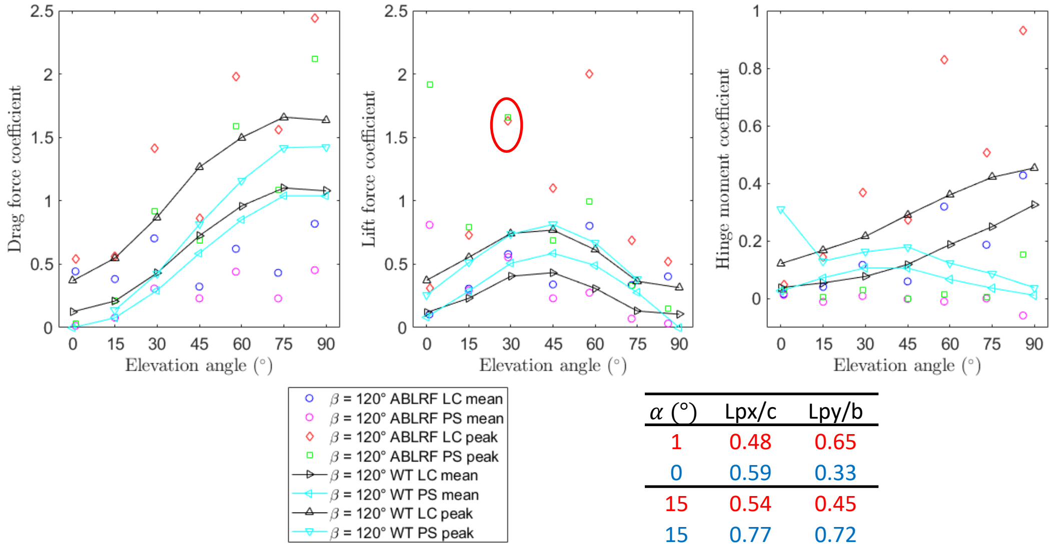

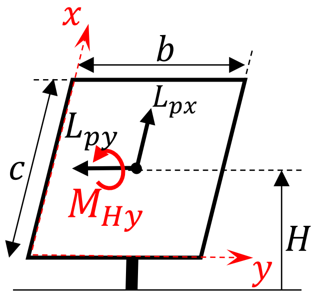

α (°)	Lpx/c	Lpy/b
1	0.48	0.65
0	0.59	0.33
15	0.54	0.45
15	0.77	0.72
29	0.48	0.49
30	0.68	0.71
45	0.50	0.46
45	0.63	0.69
58	0.52	0.41
60	0.57	0.67
73	0.50	0.43
75	0.53	0.67
86	0.63	0.41
90	0.50	0.67

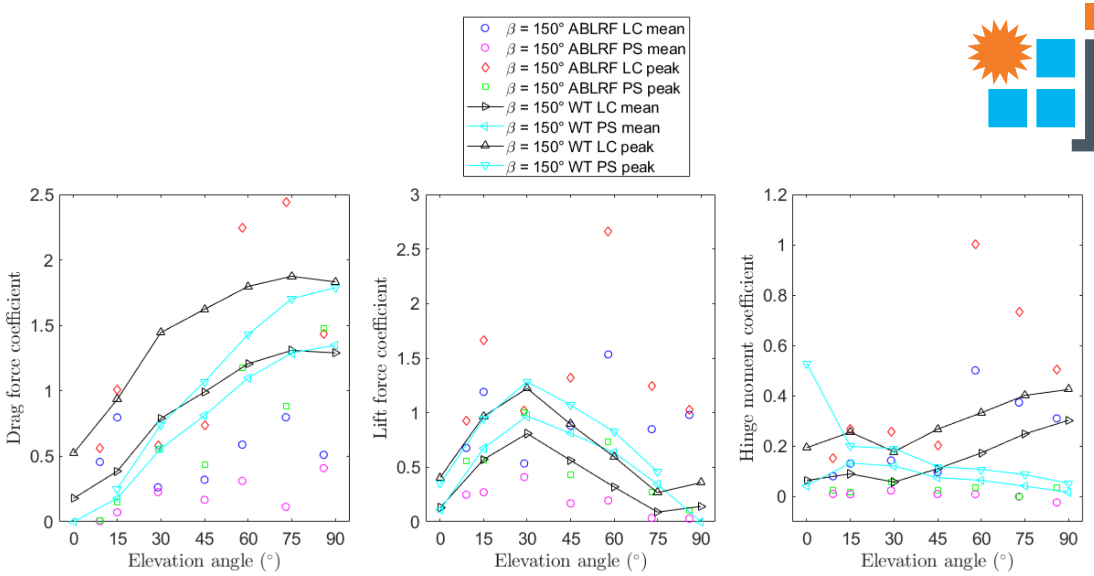

- Peak **lift force and hinge moment** at $\alpha = 29°$ ($\beta \approx 120°$) increase by factors of **2 and 1.5** respectively with decreasing I_w 16% to 11% and increasing L_w^x/c 0.4 to 0.5 at ABLRF

α (°)	Lpx/c	Lpy/b
15	0.47	0.47
15	0.69	0.64
29	0.45	0.45
30	0.61	0.60
45	0.46	0.46
45	0.57	0.58
58	0.47	0.40
60	0.55	0.58
73	0.50	0.17
75	0.53	0.58
86	0.56	0.44
90	0.51	0.59

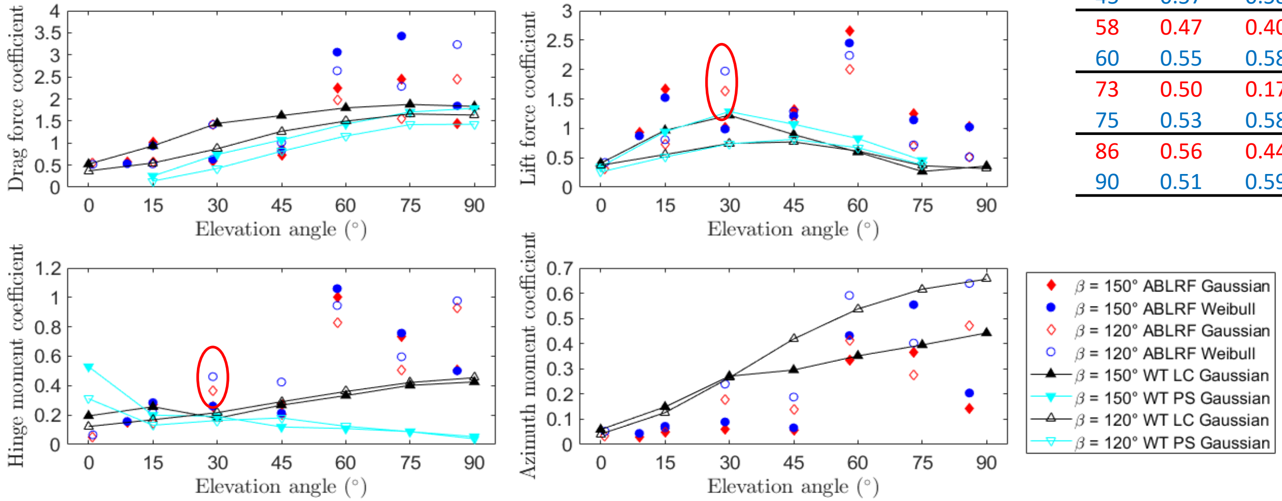

ABL Wind Analysis

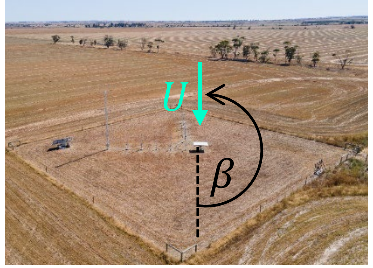

$\beta = 180°$

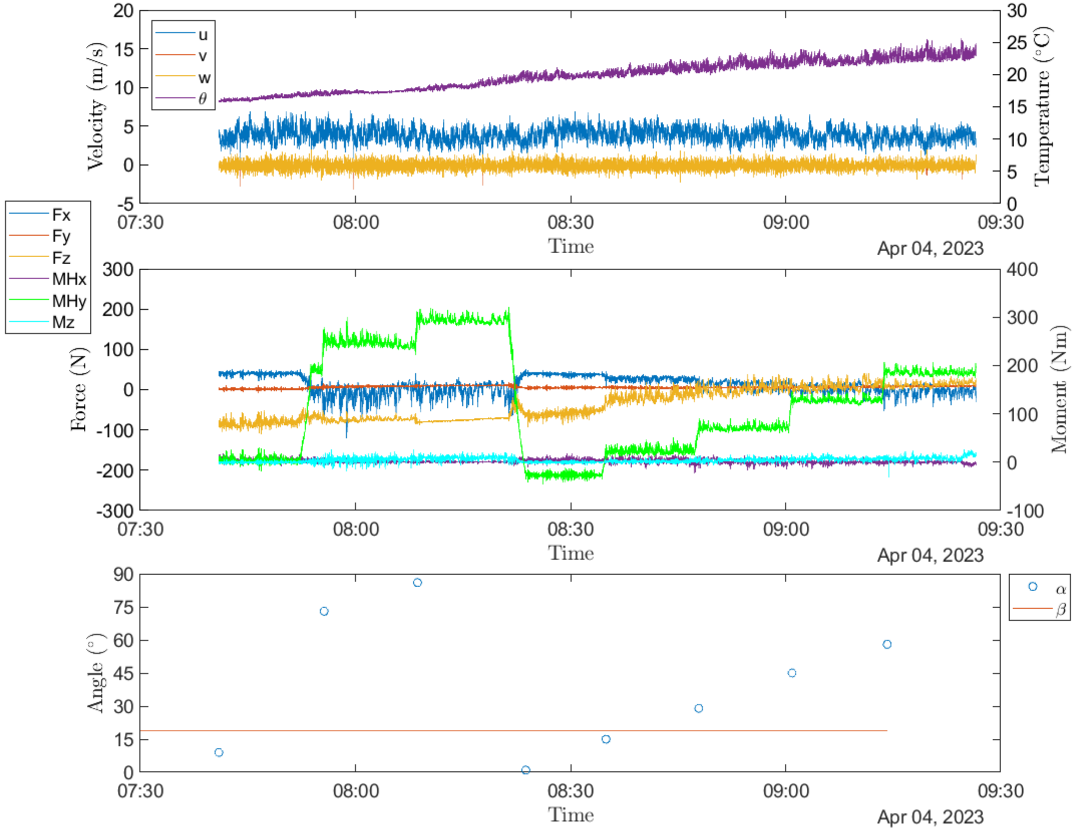

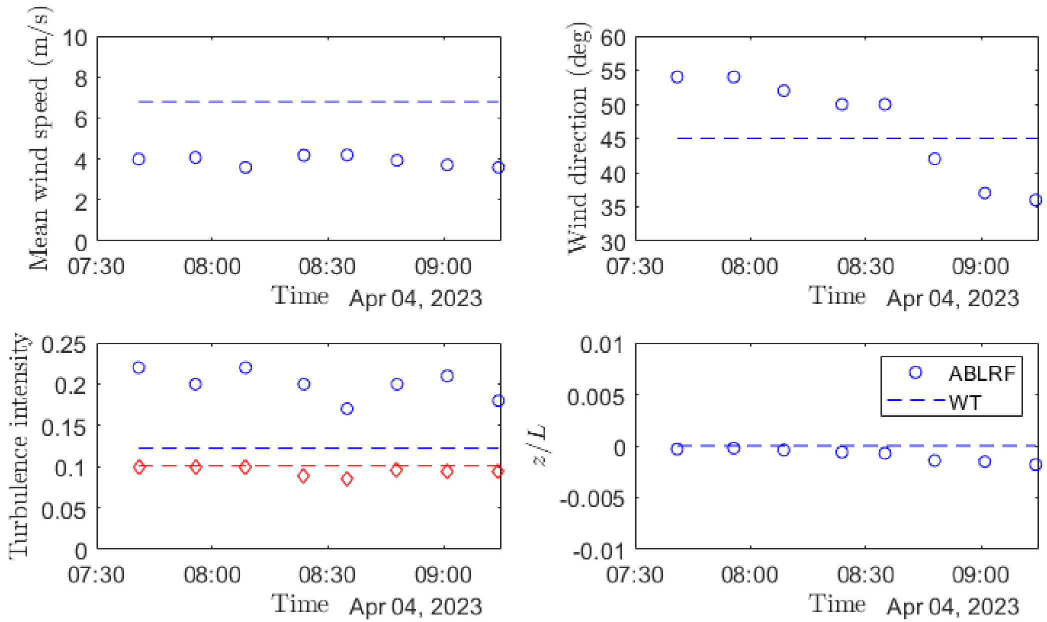

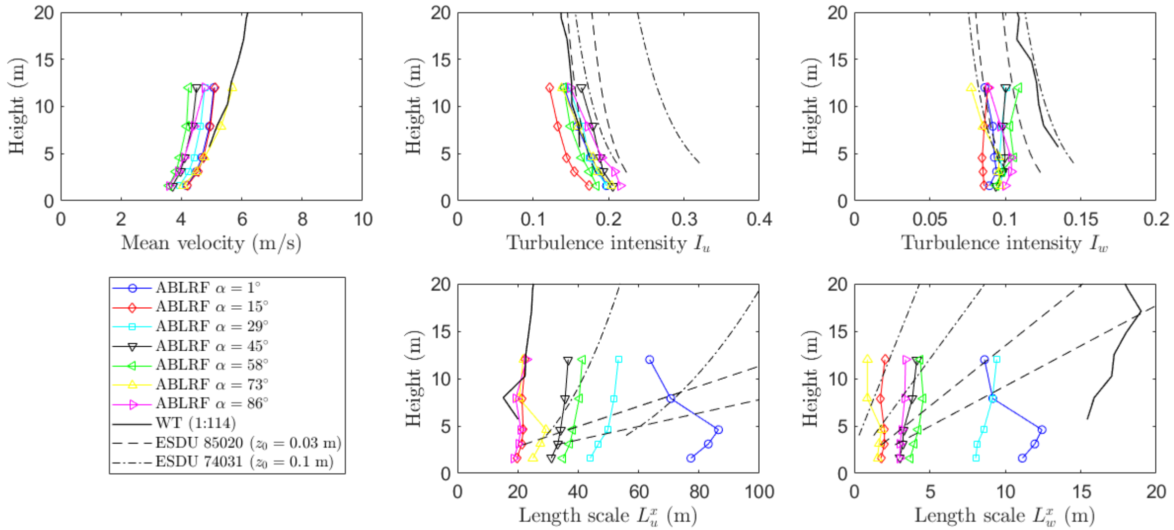

Heliostat Load Analysis

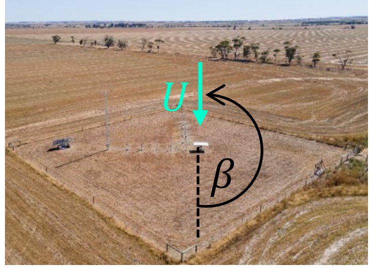

$\beta = 180°$

α (°)	Lpx/c	Lpy/b
1	0.60	0.61
0	0.52	0.75
15	0.64	0.78
15	0.64	0.51
29	0.47	0.53
30	0.57	0.51
45	0.47	0.54
45	0.57	0.51
58	0.41	0.52
60	0.56	0.51
73	0.46	0.53
75	0.53	0.52
86	0.45	0.52
90	0.51	0.52

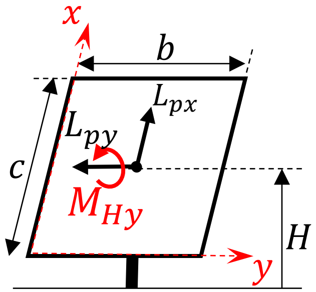

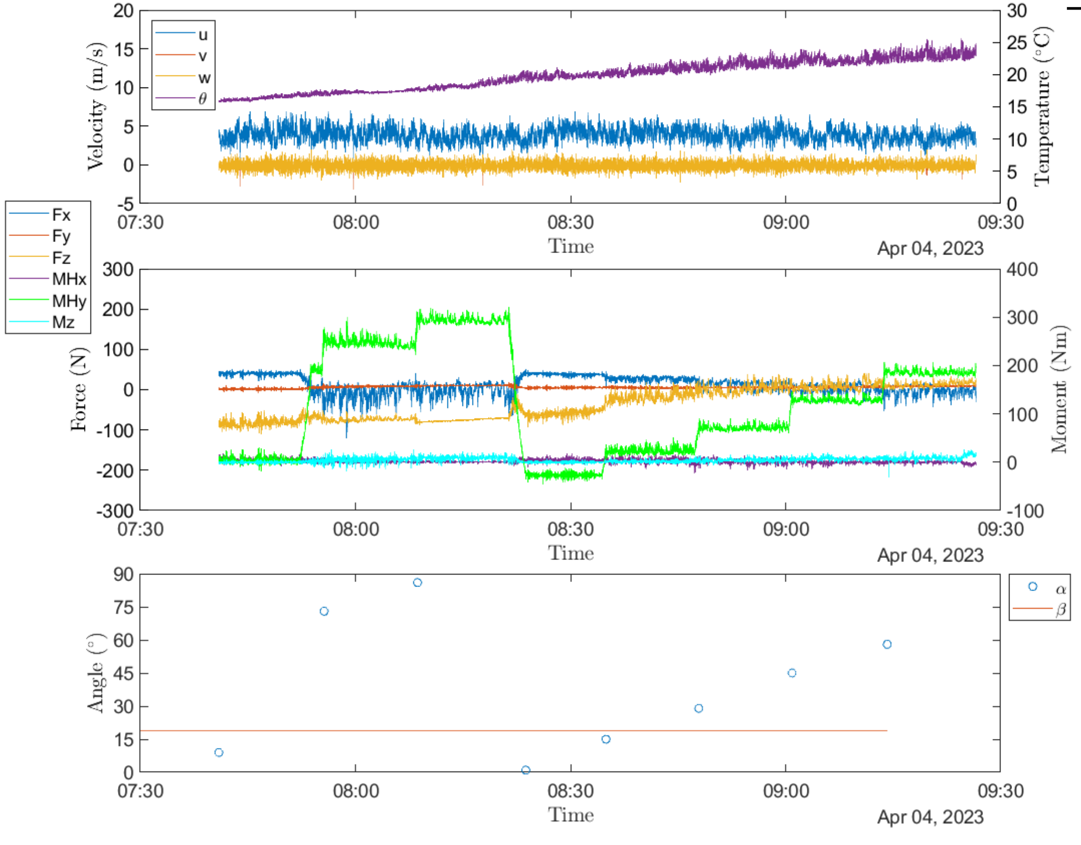

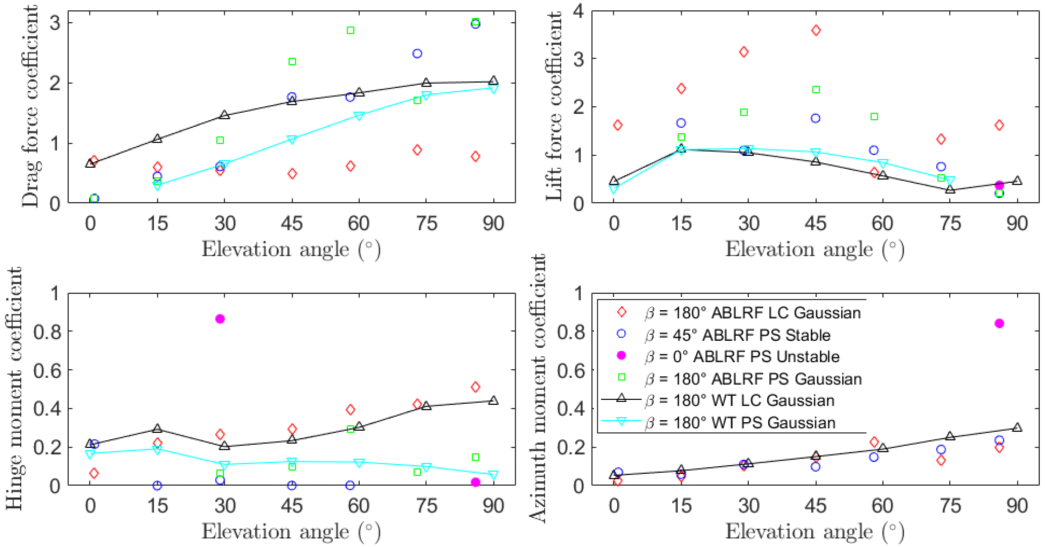

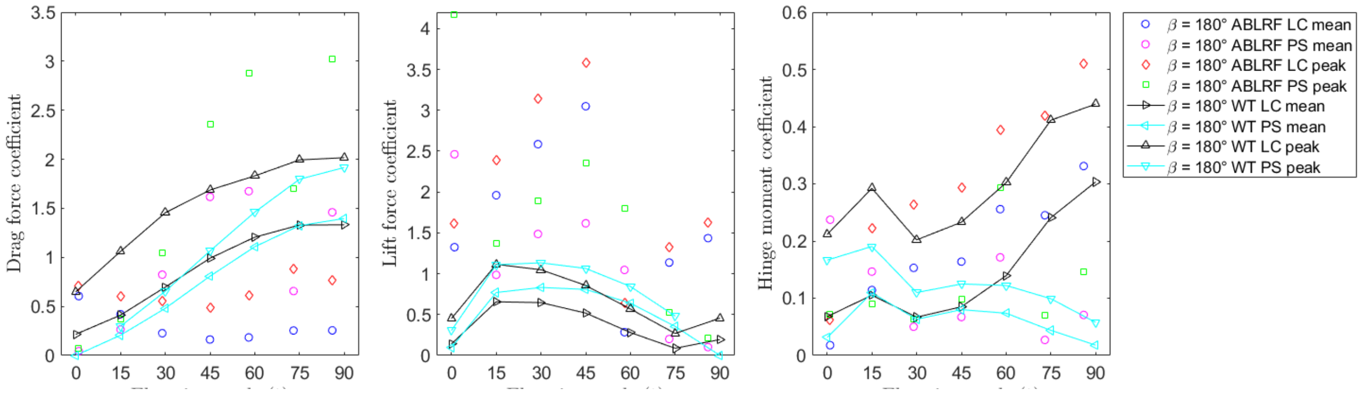

Key Takeaways

- Single heliostat wind loads are sensitive to ABL turbulence intensity and integral length scales at elevation axis height
  - Drag forces at $\alpha \geq 60°$ overestimated in wind tunnel experiments ($L_u^x/c \approx 1$) compared to field measurements ($L_u^x/c \approx 10$)
  - Lift forces at $\alpha \leq 30°$ underestimated in wind tunnel experiments ($L_w^x/c \approx 0.5$) compared to field measurements ($L_w^x/c \approx 1$)
  - Wind loads that are more sensitive to the vertical component of velocity fluctuations (i.e. lift forces and hinge moments) show a greater dependence on atmospheric instabilities, such as amplified energy of turbulence in the vertical direction during the late afternoon and evening transition
  - Azimuth moments at different β show general agreement between wind tunnel and field measurements
  - All load coefficients at ABLRF show a small to negligible variation with changes in wind speed at heliostat elevation axis height

Conclusions and Future Work

- Verification of single heliostat wind load coefficients of a 1:6 scale model in wind tunnel (WT) with field measurements
- Turbulence intensities and length scales of horizontal velocity (I_u, L_u^x) influence peak drag forces and azimuth moments, whereas vertical velocity component (I_u, L_u^x) influences peak lift forces and hinge moments
- Gaussian distribution is generally sufficient for frontal wind flow (β≈0°,180) and near-isotropic turbulence (L_u^x / L_w^x=2) in wind tunnel but can underestimate peak loads in field measurements
- Scatter and inconsistency in lift forces and hinge moments from load cell data, whereas pressure data at ABLRF is more consistent with WT data
- There is a need to unify wind load coefficient derivations using load cells and pressure sensors with shape factors applied in design standards

Acknowledgements

- Heliostat Consortium (HelioCon)

  US Department of Energy (DOE) Solar Energy Technologies Office Award DE-EE00038488/38714

- Australian Solar Thermal Research Institute (ASTRI)

  Australian Renewable Energy Agency (ARENA) Grant 1-SRI002

- Conditions over the Landscape (COtL)

U.S. DEPARTMENT OF ENERGY | Office of ENERGY EFFICIENCY & RENEWABLE ENERGY
SOLAR ENERGY TECHNOLOGIES OFFICE

NREL Transforming ENERGY

Sandia National Laboratories

ASTRI Australian Solar Thermal Research Institute

ARENA

Australian Government
Australian Renewable Energy Agency

THE UNIVERSITY of ADELAIDE

CSIRO